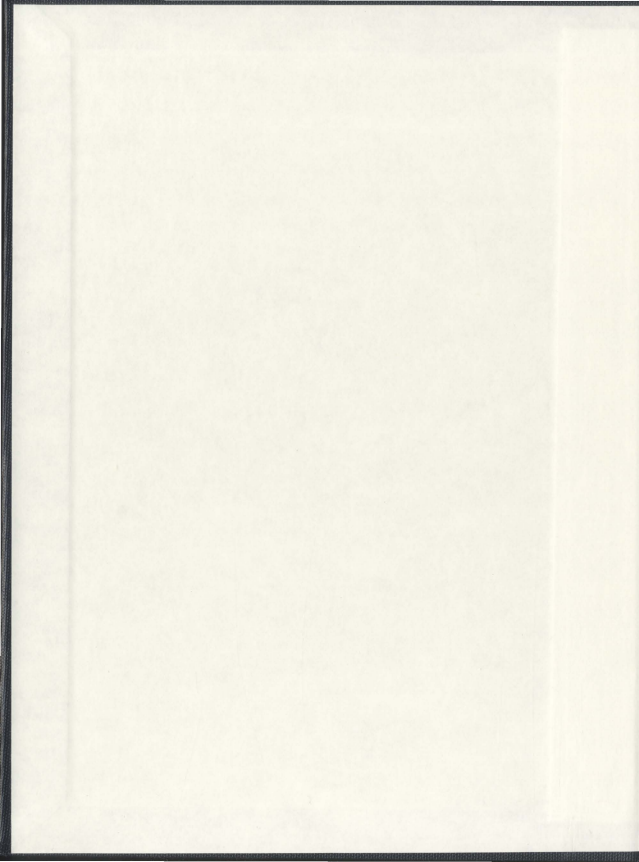


OPTIMAL RISK-BASED INSPECTION AND  
MAINTENANCE (RBIM) PLANNING FOR  
PROCESS ASSETS

MOHAMED KHALIFA





# **Optimal Risk-Based Inspection and Maintenance (RBIM) Planning for Process Assets**

By

**Mohamed Khalifa**

A Thesis submitted to the School of Graduate Studies  
in partial fulfillment of the requirements  
for the degree of Doctor of Philosophy

Faculty of Engineering and Applied Science  
Memorial University of Newfoundland

St. John's

Newfoundland and Labrador

July, 2012

## **ABSTRACT**

Process assets are subjected to deterioration during operation. Inspection is carried out at pre-defined intervals and at prescribed locations. This monitoring strategy is needed to ensure that all assets perform their intended functions and that plant integrity is not threatened. Based on the outcomes of the inspection, a maintenance decision such as repair or replacement is made.

This thesis developed a framework for optimal risk-based inspection and maintenance planning for process assets subjected to fatigue and corrosion. This framework includes two main parts:

- Inspection sampling: This part aims at estimating the required size of the inspection sample for assets/systems subjected to general corrosion and localized corrosion such as stress corrosion cracking, hydrogen induced cracking and pitting corrosion.
- Optimization of the risk-based inspection and maintenance (RBIM) plan: This part aims at determining the optimal inspection interval, inspection technique and maintenance activity (repair, replacement and/or alteration).

In the first part of the framework, the required sample size is estimated to assess general and localized corrosion of process assets/systems. In the case of general corrosion, a Bayesian approach-based method is proposed for calculating the required sample size. The proposed method ensures that the error in the posterior estimate of the mean metal loss due to general corrosion does not exceed a pre-defined acceptable margin of error at a specified confidence level. An analytical formula to estimate the sample size is introduced. The sample size obtained using the proposed method is smaller than a sample size obtained using the classical method with the same confidence level. This reduces sampling inspection cost without affecting the precision of the estimate.

In the case of localized corrosion, a different methodology is proposed to estimate the required sample size. The proposed methodology uses the extreme value and bootstrap methods. This methodology ensures that the predicted maximum localized corrosion using the extreme value method is within an acceptable margin of error at a specified confidence level. Two closed-form formulas are proposed for calculating the sample size in case of localized corrosion. The two formulas address the both situations when prior information is available or unavailable. A Bayesian updating approach is used to update prior information obtained from previously performed inspections and engineering judgement.

In the second part of the framework, a methodology for the optimal selection of an RBIM plan is proposed. This methodology is comprised of the following main steps: classification of asset's components/areas according to criticality of deterioration, asset deterioration modeling, risk assessment, cost estimation (inspection and maintenance) and finally the selection of optimal inspection intervals and a maintenance strategy. To solve the optimization problem, an objective function is formulated as a function of the present value of inspection cost, repair/replacement cost, risk of failure and the remaining value of the asset after a specified period of time. The selection of the optimum inspection interval, inspection technique and maintenance activity is based on minimizing the objective function subject to a safety constraint that the risk of failure over the lifetime of the asset does not exceed an acceptable level. The proposed methodology allows for a minimization of the inspection and maintenance cost over the lifetime of a deteriorated asset/system without compromising the safety.

The developed RBIM framework will help operators to make well informed decisions, which will result in cost effective asset integrity management and a higher level of safety.

## **ACKNOWLEDGEMENTS**

All praises are for Almighty Allah, who has given me the opportunity to accomplish this work. Throughout my PhD study and research, it has been a pleasure, working with my great colleagues and mentors and this dissertation owes much to their sincere help and encouragement.

First, I am deeply indebted to my supervisors, without them this work would not have seen the daylight: Dr. Mahmoud Haddara and Dr. Faisal Khan for offering the sparkling ideas and innovative thinking to meet the goal of research requirements for my PhD work.

My thanks are also extended to my supervisory committee member Dr. Shawn Kenny for providing instruction, comments and suggestions to improve the overall quality of the work.

I appreciate and acknowledge the financial support provided by the Natural Sciences and Engineering Research Council of Canada (NSERC), the Petroleum Research Atlantic Canada (PRAC), the Research and Development Corporation of Newfoundland and Labrador (RDC) and the Canada's research internship program administered by MITACS. I also thank the School of Graduate Studies and Faculty of Engineering and Applied Science, Memorial University of Newfoundland, for their relevant support.

Last, but not least, I would like to give my special and warmest thanks to my wife, Abeer Ahmed and my beloved kids, Hashem and Mennatullah, for their patience, sacrifices and support during my study.

## Table of Contents

ABSTRACT.....	ii
ACKNOWLEDGEMENTS .....	v
Table of Contents.....	vii
List of Tables .....	xi
List of Figures.....	xiii
List of Abbreviations .....	xvi
<b>CHAPTER 1.....</b>	<b>1</b>
Introduction.....	1
1.1. Deterioration mechanisms.....	1
1.2. Maintenance strategies.....	2
1.3. Inspection and maintenance planning approaches .....	4
1.4. Research objective .....	5
1.5. Risk-based inspection and maintenance (RBIM) approach .....	6
1.6. Literature survey .....	17
1.6.1. Inspection sampling of deteriorated assets due to corrosion .....	17
1.6.2. Risk-based inspection and maintenance .....	20
1.7. Thesis overview .....	25
<b>CHAPTER 2.....</b>	<b>27</b>
Inspection Sampling of General Corrosion- A Bayesian Approach .....	27
Abstract .....	27
2.1. Introduction.....	28
2.2. The classical method for sample size calculation .....	29
2.3. A proposed Bayesian approach-based method of sample size calculation .....	32

2.3.1.	Posterior estimate of sample mean and standard deviation .....	32
2.3.2.	Calculation of the sample size .....	35
2.4.	Case study .....	38
2.5.	Conclusion .....	47
<b>CHAPTER 3.....</b>		<b>49</b>
Inspection Sampling of Localized Corrosion- A Statistical Approach.....		49
Abstract .....		49
3.1.	Introduction.....	50
3.2.	Proposed methodology to estimate sample size for the inspection of localized corrosion.....	50
3.2.1.	Part 1- Layering separation.....	52
3.2.2.	Part 2- Physical sampling within each group.....	52
3.2.3.	Part 3- Bootstrap sampling and extreme value analysis .....	53
3.2.4.	Part 4- Calculation of the required sample size to predict the maximum localized corrosion within each group .....	61
3.3.	Analysis of variance (ANOVA).....	64
3.4.	Proposed equation to estimate sample size .....	66
3.5.	Case study .....	74
3.6.	Conclusion .....	82
<b>CHAPTER 4.....</b>		<b>84</b>
Inspection Sampling of Localized Corrosion- A Bayesian Approach .....		84
Abstract .....		84
4.1	Introduction.....	85

4.2	The proposed algorithm .....	86
4.2.1	Standard error of the standard deviation.....	88
4.2.2	Standard error of the maximum corrosion predicted using the extreme value method.....	92
4.2.3	Calculation of sample size .....	94
4.3	Prediction of the maximum localized corrosion in future time.....	101
4.4	Case study .....	103
4.5	Conclusion .....	110
<b>CHAPTER 5</b>	<b>.....</b>	<b>112</b>
	Optimization of the Risk-Based Inspection and Maintenance (RBIM) Plan .....	112
	Abstract .....	112
5.1	Introduction.....	113
5.2	The Proposed RBIM Methodology.....	113
5.2.1	Classification of asset's components/areas according to criticality of deterioration .....	115
5.2.2	Asset degradation modeling.....	115
5.2.3	Inspection and maintenance planning.....	121
5.2.4	Risk assessment .....	122
5.2.5	The expected cost of inspections over the lifetime.....	124
5.2.6	The expected cost of repairs over the lifetime.....	126
5.2.7	Optimization of the inspection intervals .....	127
5.3	Case study No. 1 .....	130
5.4	Case study No. 2 .....	140

5.5	Conclusion .....	145
<b>CHAPTER 6.....</b>		<b>146</b>
Conclusion and Future Work .....	146	
6.1.	Conclusion .....	146
6.2.	Significance and originality of the thesis .....	150
6.3.	Future work .....	151
<b>References.....</b>		<b>153</b>

### List of Tables

Table 2-1: Sample data (n =50) in mm for population size N=100.....	39
Table 2-2: Sample size and posterior sample mean for different prior standard deviations.....	42
Table 2-3: Sample size and posterior mean for different values of prior mean.....	43
Table 2-4: Sample size for different population size, N .....	44
Table 2-5: Sample data (33 data points in mm) for population size N=50.....	44
Table 2-6: Sample data (n =65) in mm for population size N=200.....	45
Table 2-7: Sample data (88 data points in mm) for population size N=1000.....	45
Table 3-1: Factors levels.....	65
Table 3-2: Comparison of the proposed equation and classical equation.....	74
Table 3-3: Recorded maximum pit depth (in mm) in 30 inspected piping segments.....	75
Table 3-4: Maximum localized corrosion in 58 inspected piping segments in mm.....	79
Table 4-1: Sample size calculation for the extreme value analysis of localized corrosion.....	101
Table 4-2: Sample size in the previous inspection for different values of population size N.....	105
Table 4-3: Sample size and the posterior estimate of the mean of the maximum corrosion size.....	106
Table 4-4: Mean and standard deviation of the maximum corrosion size over the population ( $x_{\max,\Delta t}$ and $\sigma_{x_{\max,\Delta t}}$ ) for different periods of time after the current inspection ( $\Delta t$ ).....	110

Table 5-1: The optimum inspection schedule for plan A (case study No. 1) .....	136
Table 5-2: The optimum inspection schedule for plan B (case study No. 1).....	139
Table 5-3: The optimum inspection schedule (case study No. 2).....	144

## List of Figures

Figure 1-1: RBIM planning.....	8
Figure 1-2: An example of semi-quantitative risk matrix.....	16
Figure 1-3: Thesis organization.....	25
Figure 2-1: Normal probability plot of sample data shown in Table 2-1.....	40
Figure 2-2: Sample size, $n$ , for different population size, $N$ .....	46
Figure 2-3: Percentage of saving when using the proposed formula in comparison to the classical formula for different population size, $N$ .....	47
Figure 3-1: Proposed methodology flowchart.....	51
Figure 3-2: Bootstrapping to estimate standard error and confidence intervals.....	57
Figure 3-3: Extrapolation of Gumbel probability plot to predict the maximum localized corrosion over the entire population.....	60
Figure 3-4: COE <sub>mean</sub> versus bootstrap sample size, $n_b$ , for population size, $N = 100$ .....	68
Figure 3-5: Bootstrap sample size, $n_b$ , versus COE <sub>max</sub> .....	70
Figure 3-6: Predicted versus actual COE <sub>max</sub> .....	72
Figure 3-7: Gumbel probability plot of the inspection data.....	76
Figure 3-8: COE <sub>max</sub> versus bootstrap sample size for population size of 100.....	77
Figure 3-9: COE <sub>max</sub> versus sample size for population size of 1000.....	81
Figure 4-1: The flowchart of the proposed algorithm.....	87
Figure 4-2: A procedure to obtain an approximate formula to estimate standard error of standard deviation.....	89
Figure 4-3: Using bootstrap sampling to validate the obtained approximate formula to estimate standard error of standard deviation.....	91

Figure 4-4: $SE_{Std, Gumbel}$ obtained with the proposed formula (Eq. 4.5) versus $SE_{Std, Gumbel}$ obtained with bootstrap simulation.....	92
Figure 4-5: The corrosion rate estimation with the extreme value method as suggested by Kowaka et al. (1984).....	98
Figure 4-7: The margin of error, MOE, and the upper limit of the posterior estimate of the maximum corrosion at a confidence level of 95%.....	108
Figure 5-1: The proposed methodology flowchart. ....	114
Figure 5-2: Inspection intervals as a fraction of the remaining life.....	122
Figure 5-3: Simulation of the flaw size growth with time (after Chung et al., 2006)....	125
Figure 5-4: Cost (inspection and repair), risk of failure and objective function versus different values of R for a suggested inspection and maintenance plan. ....	130
Figure 5-5: The net present values of the cost (inspections cost and repairs cost) for different values of R (plan A). ....	134
Figure 5-6: The net present values of risk of failure for different values of R (plan A). 134	
Figure 5-7: The net present value of the objective function for different values of R (plan A). ....	135
Figure 5-8: The net present value (NPV) of the cost (inspections cost and repairs cost) for different values of the ratio R (plan B). ....	137
Figure 5-9: The net present value (NPV) of the risk of failure for different values of the ratio R (plan B). ....	137
Figure 5-10: The net present value (NPV) of the objective function for different values of the ratio R (plan B). ....	138

Figure 5-11: The effect of failure cost ( $K_F=10^7$ ) on the optimal selection of RBIM plan.....	140
Figure 5-12: The net present values of the cost (inspections cost and repairs cost) for different values of R.....	142
Figure 5-13: The net present values of risk of failure for different values of R.....	143
Figure 5-14: The net present value (NPV) of the objective function for different values of the ratio R.....	144

## List of Abbreviations

$a_o$	Initial crack/flaw size
$a_p$	Pit depth
$a_r$	Crack size which should be repaired
$a_{N_C}$	Crack size after $N_C$ stress cycles
$A(a_i)$	Probability of acceptance of crack with size $a_i$ at the $i$ th inspection
ANOVA	Analysis of variance
API	American Petroleum Institute
ASTM	American Society for Testing and Materials
C and m	Material parameters for fatigue crack growth rate
CI	Confidence interval
$C_l$	Expected cost of inspections over the lifetime
COEmax	Coefficient of error of the maximum
COEmean	Coefficient of error of the mean
COV	Covariance
CR	Corrosion rate
$c_r$	Cost of repair over the lifetime in a simulation of the flaw growth
$C_R$	Expected cost of repairs over the lifetime
$C_{Repl}$	Replacement cost

$da/dt$	Crack growth rate
$F(x)$	Cumulative density function of $x$
$F(x_{\max})$	Cumulative density function of $x_{\max}$
FPB	Finite population bootstrap
FPCF	Finite population correction factor
HIC	Hydrogen induced cracking
K	Crack tip stress intensity factor
$k_F$	Cost of failure
$k_I$	Cost of one inspection
$k_R$	Cost of one repair
$K_{th}$	Crack tip stress intensity factor threshold
$MOE_{accept}$	Acceptable margin of error
$MOE_{max}$	Margin of error of the maximum corrosion size over the entire population
$MOE_{mean}$	Margin of error of the mean
MVCF	Maximum value correction factor
N	Population size
n	Sample size in the current inspection
$n_o$	Sample size in the previous inspection
$n_b$	Bootstrap sample size
$N_C$	Number of stress cycles
$N_{cr}$	Critical number of stress cycles

$N_j$	Number of inspections before reaching the critical time to failure in the jth simulation
NPV	Net Present Value
$N_{\text{sim}}$	Number of simulations
OF	Objective Function
POD( $a_i$ )	Probability of detection of a flaw with size $a_i$ in the ith inspection
POE	Probability of Exceedance
PRA	Probabilistic Risk Assessment
R	Inspection interval as a fraction of the remaining life
r	Discount rate
RBIM	Risk-based inspection and maintenance
$R_V$	Remaining value after a defined period T (study period)
s	Scale parameter
SCC	Stress corrosion cracking
$SE_{\max}$	Standard error of the maximum corrosion size over the population
$SE_{\text{mean}}$	Standard error of sample mean
$SE_{\text{std}}$	Standard error of sample standard deviation
t	Time
T	Study period
$t_{\alpha}$	Critical time to failure
$t_i$	Time of the ith inspection
$t_{\text{int}}$	Inspection interval between the current and previous inspections

$t_{\text{Repl}}$	Time of replacement
$x$	Maximum corrosion size in each inspected component/area
$x_{\max}$	Maximum corrosion size over the asset/system (population)
$Y(a)$	Geometry function
$Y_{\text{av}}$	Average geometry function
$\alpha$	Significance level
$\gamma$	Euler constant
$\Delta k$	Stress intensity range factor
$\Delta \sigma$	Applied stress range
$\Delta \sigma_{\text{eff}}$	Effective stress range
$\theta$	Scale parameter
$\beta$	shape parameter
$\lambda$	Location parameter
$\mu$	Population mean of the corrosion size
$\mu'$	Prior mean of the corrosion size
$\mu_s$	Sample mean of the corrosion size
$\mu''_{\mu s}$	Posterior mean of $\mu_s$
$\sigma$	Population standard deviation of the corrosion size
$\sigma'$	Prior standard deviation of the corrosion size
$\sigma''_{\mu s}$	Posterior standard deviation of $\mu_s$
$\sigma'_{\mu s}$	Prior standard deviation of $\mu_s$

$\sigma_s$	Sample standard deviation of the corrosion size
$x_{\max}$	Predicted maximum corrosion size over the population in the current inspection
$x_{\max,\Delta t}$	Maximum corrosion size over the population after a period of time $\Delta t$
$x'_{\max}$	Prior mean of $x_{\max}$
$x''_{\max}$	Posterior mean of $x_{\max}$
$x^0_{\max}$	Predicted maximum corrosion size over the population in the previous inspection
$x^{0\prime}_{\max}$	Posterior mean of $x^0_{\max}$
$\sigma_{x_{\max}}$	Standard deviation of $x_{\max}$
$\sigma_{x_{\max,\Delta t}}$	Standard deviation of $x_{\max}$ after a period of time $\Delta t$
$\sigma'_{x_{\max}}$	Prior standard deviation of $x_{\max}$
$\sigma''_{x_{\max}}$	Posterior standard deviation of $x_{\max}$
$\sigma^0_{x_{\max}}$	Standard deviation of $x^0_{\max}$
$\sigma'_{x^0_{\max}}$	Prior standard deviation of $x^0_{\max}$
$\sigma''_{x^0_{\max}}$	Posterior standard deviation of $x^0_{\max}$
$\sigma_{CR}$	Standard deviation of the corrosion rate

## **CHAPTER 1**

### **Introduction**

#### **1.1. Deterioration mechanisms**

Processing plants' assets such as pipelines, vessels, tanks, towers, boilers, heat exchangers and heaters are subjected to several structural deterioration mechanisms during their operation. Structural deteriorations may result in damage, deformation, defects or performance degradation. The most common deterioration mechanisms are:

- a) Corrosion

Corrosion results in metal loss, pitting, cracks or/and degradation of material properties due to changes in the material microstructure. Corrosion could be general or localized. General corrosion is a metal loss widely distributed over the surface area of an asset. Localized corrosion results in a localized metal loss or cracks at different small areas over the material surface such as pitting corrosion, galvanic corrosion, crevice corrosion, stress corrosion cracking and Hydrogen induced cracking.

b) Fatigue

Fatigue occurs due to fluctuating stress (mechanical fatigue) or fluctuating temperature (thermal fatigue). Fatigue causes initiation and growth of cracks especially at locations of material discontinuities until the crack size reaches a critical limit such that the asset is no longer able to resist the applied load.

c) Creep

Creep is continuous plastic deformation that happens when an asset is continuously subjected to a load for a long time. Creep deformation is accelerated at high temperatures. Creep is accompanied by microscopic voids that eventually lead to macroscopic cracks and crack growth.

d) Corrosion-fatigue-creep interaction

An asset could be subjected to combined degradation mechanisms such as corrosion, fatigue and creep. The degradation is accelerated due to the presence of several mechanisms at the same time.

## **1.2. Maintenance strategies**

Maintenance activities such as repair, replacement and alteration may be required as a follow up to inspection. Repair refers to work that is necessary to

restore an asset to a state at which it is able to perform its intended function according to the design conditions. Alteration involves a physical change which improves the ability of an asset to perform its intended function. A change in operating conditions such as temperature or pressure is not an alteration and is referred to as re-rating.

Maintenance can be classified as:

- a) Preventive maintenance

Preventive maintenance consists of maintenance tasks which attempt to preempt failure of an asset.

Preventive maintenance can be sub-divided into:

- Scheduled maintenance

Scheduled maintenance is carried out at prescribed intervals of time to ensure that an asset is operating correctly and to avoid any unscheduled downtime.

- Predictive (condition-based maintenance).

Predictive maintenance is based on the use of a physical parameter or characteristic of an asset such as vibration, temperature, pressure, voltage, current, sound, colour or resistance to detect major changes in the performance of the

asset. Measurements of the parameter are made either continuously or at regular intervals and the results are compared with initial measurements made when the asset was new. A certain limit, for the amount of acceptable deviation from as new condition, is decided at the beginning of the maintenance cycle. A repair or replacement action is then performed prior to the anticipated time of failure.

b) Reactive maintenance (corrective maintenance)

Reactive maintenance is carried out after the occurrence of failure in order for an asset to return to its operating condition. This type of maintenance is useful when the cost of the failure consequences is lower than the preventive maintenance cost.

### **1.3. Inspection and maintenance planning approaches**

In-service inspection and maintenance could be planned based on one of the following approaches:

- i) Remaining life-based approach: The remaining life approach is based on calculating the remaining life of an asset according to its tolerance to deterioration, defects or damage and the rate of deterioration. The tolerance to deterioration is determined by assessing fitness-for-service at future times according to the deterioration predicted. The interval between two

consecutive inspections equals a fraction of the remaining life. The remaining life is assessed based on analytical fracture mechanics models such as Paris's equation for fatigue crack growth rate or based on statistical methods to estimate the corrosion rate using the history obtained from previous inspections.

- ii) Reliability-based approach: The inspection and maintenance are planned such that the reliability of the asset remains greater than previously determined target reliability. Reliability centered maintenance (RCM) is a typical example of this approach.
- iii) Risk-based approach: The inspection and maintenance activities are planned based on maintaining the risk of failure below an acceptable level. RBIM is a typical example of this approach.

#### **1.4. Research objective**

To develop a framework for optimal risk-based inspection and maintenance of process assets subjected to fatigue and corrosion. This framework includes two main parts:

- Inspection sampling: This part aims to estimate the required sample size for inspection of process systems subjected to general corrosion

and localized corrosion such as stress corrosion cracking, hydrogen induced cracking and pitting corrosion.

- Optimization of the risk-based inspection and maintenance (RBIM) plan: This part aims to select the optimal inspection interval and maintenance strategy.

### **1.5. Risk-based inspection and maintenance (RBIM) approach**

Risk-based inspection and maintenance (RBIM) is a strategy which aims at maintaining the integrity of a plant or an asset that is subjected to deterioration. Maintaining the asset integrity guarantees maintaining the risk of failure below an acceptable level.

Although RBIM reduces risk of failure of a plant subjected to deterioration during its operation, failure may still occur as a result of incorrect design, manufacturing defects, or extreme environmental random events.

Thus, to ensure the integrity of a plant, all the following requirements should be satisfied:

- a) Proper design procedures should be followed to ensure that all assets are able to withstand the applied loads. Appropriate design approach should be followed and relevant codes and regulations should be consulted.

- b) A system for quality assurance should be in place to eliminate manufacturing defects.
- c) An inspection and maintenance plan to ensure the integrity of all assets during operation should be implemented.

RBIM is a team activity. Technical knowledge and experience should include the following:

- a) Risk assessment
- b) Plant potential hazards, damage mechanisms and failure consequences
- c) Plant safety
- d) Material and corrosion engineering
- e) Plant operation and maintenance
- f) Inspection techniques and inspection history.

#### **1.5.1. Steps of RBIM planning**

Figure 1-1 summarises the steps of RBIM plan. The details of each step are explained in sub-sections 1.5.1.1 through 1.5.1.5.

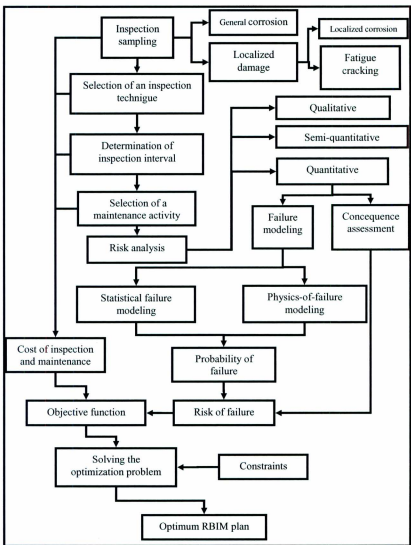


**Figure 1-1:** RBIM planning.

### ***1.5.1.1. Inspection sampling***

In-service inspection is employed to evaluate the condition of process assets. Often, it is impractical to inspect the large number of components that constitute a complete asset. Therefore, inspection sampling is carried out where preselected components or areas are inspected. In this case, it is required that the results obtained from the sample best represent the condition of the asset (population).

In case of general corrosion, determination of the mean metal loss is required to evaluate the condition of the population. While in case of localized corrosion, the maximum corrosion flaw size over the entire population is to be determined because the failure will occur when the maximum localized corrosion reaches a critical size at any location. In other words, the objective of inspection sampling is to evaluate the mean of the metal loss in case of general corrosion and to evaluate the maximum corrosion flaw in case of localized corrosion.

Chapters 2, 3 and 4 illustrate how inspection sampling is applied for assets which suffer from either a general metal loss (i.e, general corrosion) or a localized corrosion. The analysis can also be extended to other forms of deterioration.

#### *1.5.1.2. Selection of inspection technique and schedule*

An inspection plan involves selection of an inspection technique and inspection schedule.

Different non-destructive inspection techniques are used for in-service inspection such as ultrasonic, radiographic, eddy current and magnetic techniques. Selection of the best technique to be used depends on the ability of the technique to detect the damage, cost of performing the inspection using this technique, and the risk of failure. This selection could be based on expert subjective judgement or on quantitative basis.

Inspections are usually scheduled at specified times. Inspection times are chosen based on two factors. The first factor is reducing the risk of failure to an acceptable level. The second factor is the cost of the inspection.

#### *1.5.1.3. Selection of a maintenance activity (repair, replacement and/or alteration)*

The condition of the inspected asset will dictate the maintenance action that will be taken. The asset may be repaired, replaced, or left as is depending on its condition. The action taken is based on the acceptable risk of failure of the asset to perform its intended function until the next inspection. The maintenance cost is

also a factor when deciding the action to be taken. A balance between the cost of inspection and maintenance can be achieved in the last step (optimization of the RBIM plan).

#### *1.5.1.4. Risk assessment*

Risk is expressed as the product of the consequences of failure or an undesired event and the probability of its occurrence.

Risk can be assessed using qualitative, quantitative or semi-quantitative approaches.

##### a) Qualitative approach

Qualitative risk assessment relies on subjective judgement. The probability and consequences of failure are expressed in descriptive and relative terms. For example terms like, very unlikely, possible, reasonably probable and probable can be used to describe the likelihood of failure. The consequence of failure may be described as high, moderate, low. The qualitative approach provides an easy and quick method for the assessment of risk. Its disadvantage is that the evaluated risk is subjective and therefore the links to mitigation activities are also subjective.

b) Quantitative approach

Quantitative assessment relies on the availability of data. It requires the determination of a specific value for the probability of failure based on probabilistic analysis (not based on subjective judgment) and the determination of a quantitative estimate for the consequences of failure.

An advantage of this approach is that it allows the benefits of the risk mitigation activities to be quantified. This approach requires long time for data recording and analysis. It also requires failure modeling and failure consequences assessment. Failure modeling deals with formulating failure models to predict failure occurrences and to evaluate probability of failure. Two approaches may be used to model the failure:

i. Statistical failure modeling approach

This approach is based on the use of statistical failure data to determine the instantaneous failure rate (hazard function) as a function of time. The probability distribution of time to failure is obtained and the probability of failure is estimated. In this approach, the failure is considered as function of time only without looking at the physical factors or reasons which affect failure. For details of this approach see Ebeling (1997).

## ii. Physics-of-failure modeling approach

In many applications, the failure of an asset may depend on some variables such as materials properties, damage size, loading, and operating and environment conditions. A more accurate failure model may be one in which these variables are considered. This approach is based on the availability of accurate analytical models to describe the failure of an asset subjected to different degradation mechanisms. This approach requires less data in comparison to the statistical approach. These analytical models are expressed in terms of the variables that affect failure. These variables are in general random. Therefore, this approach can be combined with statistical methods to model the failure. Models obtained using probabilistic fracture mechanics are typical examples of this approach. For example, Paris's equation (1963) for modeling the fatigue crack growth rate can be used with a distribution of crack size to estimate the probability of failure of an asset subjected to fatigue.

In physics-of-failure modeling approach, the probability of failure of a deteriorated asset can be expressed as the probability that the limit state function,  $G$ , is less than zero. The limit state function,  $G$ , is defined as the resistance or strength minus the load or stress. Resistance of an asset subjected to deterioration

depends on the material properties in a specified environment, asset dimensions and damage size. Load depends on the operation and environment conditions.

The consequence of an asset failure could include physical injury to personnel in the vicinity and cause structural damage to surrounding assets. It also could cause production loss due to shut down. The contaminants of the asset may be released due to failure. The release could have the potential for one or a combination of the following events:

i) Flammable releases

When flammable releases meet with a source of ignition, a fire will result at a close range but an explosion may reach over a large range from the centre of the release.

ii) Steam and hot gas releases

Steam and hot gas releases can result in very severe injury or burns to people within range.

iii) Toxic releases

The dispersion of toxic releases may extend over large distances from the site. Employees, the general public and the environment may be affected.

iv) High pressure gas release

High pressure gas release has the potential to cause physical injury to personnel in the vicinity and cause structural damage to surrounding assets.

Finnaly, the quantitative risk is assessed as multiplication of probability of failure and consequences of failure.

c) Semi-quantitative approach

In the semi-quantitative risk assessment, numerical values for the probability of failure and the consequences are assumed on the basis of expert judgment using available estimates for similar assets. Then, the tools which are used in the quantitative assessment approach such as the fault tree and event tree can be used to evaluate the system probability of failure using a subjective probability of failure of each asset. Thus, it can be said that the semi-quantitative risk assessment is a combination of the qualitative and quantitative assessments. It does not require as much data as needed for the quantitative approach. In the semi-quantitative risk assessment approach, factors which may affect the probability of failure and the consequences are weighted or given scoring points (for example from 0-100) based on expert judgement. The sum of the weights or the scoring points gives an indication of the level of the probability of failure and the consequences of failure. The level of the probability of failure and its consequences can be classified into

categories (from the lowest to the highest) and is usually represented in the form of a semi-quantitative risk matrix. The risk level is evaluated as the product of sum of weighting factors (or scoring points) of each the probability of failure and consequences. An example of a semi-quantitative risk matrix is shown in Figure 1-2.

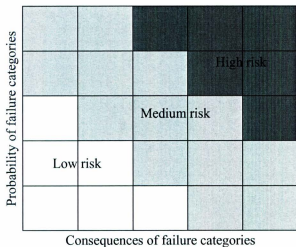


**Figure 1-2:** An example of semi-quantitative risk matrix.

The inspection plan for each item is then prioritized based on the risk level in the risk matrix.

### *1.5.1.5. Optimization of the RBIM plan*

Different inspection and maintenance plans are suggested. The basis of selecting the optimal RBIM plan is determined, for example, minimizing the risk of failure, maximimizing the risk reduction as a result of carrying out the inspection and maintenance activities or minimizing inspection and maintenance cost while maintaining risk of failure below an acceptable level. An objective function is formulated and the optimization problem is solved on the determined basis.

## **1.6. Literature survey**

Leterature survey has been carried out to cover the two main parts of the framework. Many studies which address risk-based inspection and maintenance planning are available in the open literature. Meanwhile, few literature address inspection sampling of deteriorated assets due to corrosion.

### **1.6.1. Inspection sampling of deteriorated assets due to corrosion**

When a part of a deteriorated asset is subjected to the same operating and corrosion conditions, a representative sample is inspected from this part. For example, a segment of a pipeline could be subjected to the same operating and

corrosion conditions. A sample (number of components or areas) of this pipeline segment is inspected.

API 570 (piping inspection code) provides excellent recommendations for conducting good piping inspections; however, it does not provide specific guidelines to determine the inspection sample size. In API 570, inspection sample size is left for the inspection practitioner's judgment (Hobbs and Ku 2002).

API 580/581 (risk-based inspection) considers risk as a basis for inspection planning. Although API 580/581 provides guidance for determining frequency of inspections, it does not provide specific guidance for determining minimum number of locations to be inspected to represent the condition of the complete system.

The corrosion rate and mean of the metal loss are enough to assess general corrosion. As the size of the metal loss due to general corrosion can be modeled by normal distribution and the required parameter to be evaluated is the mean metal loss; the classical method (Eqs 2-3 and 2-4) for estimating sample size from a normally distributed population can be used.

In case of localized corrosion, the maximum corrosion size is to be evaluated because the failure may occur at any location at which the corrosion size is greater than a critical size (Kowaka et al., 1984). Thus, the strategy of sampling should

be different when sampling from components/areas subjected to localized corrosion than general corrosion. For localized corrosion, there is a lack of studies aim to address sample size and no clear consensus on this problem but it is widely believed that the larger the sample size is the smaller the error of the sample estimate (Kowaka et al., 1984 and Alfonso et al., 2008). This problem was studied previously by Shibata (1991), Schneider et al. (2001), Wang (2006) and Alfonso et al. (2008). Shibata (1991) showed from historical data that localized corrosion maybe modeled with Gumbel extreme value distribution with location parameter ( $\lambda$ ) and scale parameter (s) change with time while the ratio ( $s/\lambda$ ) remains approximately constant irrespective of the time for a certain material in same environment. Shibata (1991) plotted sample size (n) versus return period (T) for different ratios ( $s/\lambda$ ) estimated using the minimum variance linear unbiased estimator method. From this plot, the optimum sample size is obtained for a given return period. Schneider et al. (2001) estimated the required inspection area by investigating the dependence between the data points at different distances from each other. Wang (2006) estimated the required number of tubes in heat exchangers for the assessment of the minimum remaining thickness of tubes in industrial heat exchangers subjected to corrosion. Alfonso et al. (2008) aimed to estimate the optimum sample size and unit inspection area in a long pipeline based on the required accuracy of the estimate of maximum pit depth in un-pigable,

buried pipelines using the extreme value method. Alfonso et al. (2008) performed extensive Monte Carlo simulations to estimate the mean square error of the estimate of the maximum localized corrosion as an indicator to the estimate accuracy for different sample sizes.

When an asset is subjected to fatigue, critical fatigue locations can be determined based on stress analysis (Zhou et al., 2007). A sample of locations/components is inspected from each group of similar criticality to fatigue.

#### **1.6.2. Risk-based inspection and maintenance**

Vaurio (1995) presented a procedure for optimizing test and maintenance intervals of safety related systems and components. The method is based on minimizing the total plant-level cost under the constraint that the total accident frequency remains below a set criterion.

Nessim and Stephens (1995) presented a risk based methodology that estimates the optimal maintenance interval for an aging hydrocarbon pipeline network. The presented risk based maintenance methodology consists of two main steps: to rank different segments of the pipeline according to priority for maintenance, and to select an optimal set of maintenance actions for the chosen segments.

Balkey et al. (1998) developed a methodology, which includes risk based ranking methods, beginning with the use of plant probabilistic risk assessment (PRA), for the determination of risk-significant and less risk-significant components for inspection and the determination of similar populations for pumps and valves for in-service testing. This methodology integrates non-destructive examination data, structural reliability/risk assessment results, PRA results, failure data and expert opinions.

Apeland and Aven (2000) developed a risk based maintenance optimization approach. The optimal strategies are determined by evaluating the relationship between the benefits associated with each maintenance alternative and its cost.

Wintle et al. (2001) provided guidelines including the best practice for risk based inspection as a part of plant integrity management.

Faber (2002) explained a framework for risk-based inspection including probability and consequence of failure assessment, modelling of uncertainties, modelling of deterioration processes and acceptance criteria for RBI.

Kallen (2002) developed a probabilistic risk-based inspection methodology. This methodology used a stochastic process to model the corrosion damage mechanism and to develop optimal inspection plans. Cost functions associated with a Gamma process for modeling deterioration are developed.

Misewicz et al. (2002) developed a risk based integrity project ranking approach for natural gas and CO<sub>2</sub> pipelines. The approach is based on a benefit cost ratio, defined as the expected risk reduction in dollars per mile over the project useful life, divided by the total project cost. Risk reduction is estimated using a quantitative risk analysis approach. The benefit cost ratio results can be used as a tool to justify the maintenance budget.

Khan and Haddara (2003) presented a risk-based maintenance methodology for designing an optimum inspection and maintenance programs. The methodology consists of three modules: risk estimation, risk evaluation and maintenance planning. Each module consists of many steps; for example, risk estimation module involves: (i) failure scenario development, (ii) consequence assessment, (iii) probabilistic failure analysis, and (iv) risk estimation.

Kallen and Noortwijk (2004) presented a risk-based inspection (RBI) technique that develops cost and safety optimal inspection plans. Bayesian decision model is used to determine these optimal inspection plans under uncertain deterioration. The presented risk-based inspection technique uses the Gamma stochastic process to model the corrosion damage mechanism and Bayes' theorem to update prior knowledge over the corrosion rate with imperfect wall thickness measurements. A periodic inspection and replacement policy which minimizes the

expected average costs per year is found. An example using actual plant data of a pressurized steel vessel is presented.

Krishnasamy et al. (2005) developed a risk-based inspection and maintenance methodology for a power generating plant. Applying this methodology reduces risk, increases the reliability of assets, and reduces the cost of maintenance.

Khan et al. (2006) proposed a RBIM methodology uses a gamma distribution to model the material degradation and a Bayesian updating method to improve the distribution based on actual inspection results. The methodology optimizes maintenance intervals based on a level of risk that satisfies the acceptable risk criteria.

Santosh et al. (2006) proposed a mathematical model to estimate the reliability of pipelines containing corrosion defects due to H<sub>2</sub>S for the purpose of risk-based inspection.

Khan and Howard (2007) presented a simplified practical approach for the use of statistical tools for inspection planning and integrity assessment. The study is focused on corrosion related material degradation of piping on an offshore production facility.

Khalifa et al. (2009) proposed a methodology for the optimal selection of a non-destructive inspection (NDI) technique and its associated in-service inspection interval for welded components subjected to cyclic loading fatigue. An objective function is formulated in this methodology as sum of the inspection cost, the repair cost and the risk of failure. The optimum inspection interval and non-destructive inspection technique are selected by minimizing the objective function taking into account a safety constraint that the probability of failure does not exceed an acceptable level.

Zhao (2009) applied the risk matrix of API 581 (2000) for risk-based inspection of High-Pressure Hydrogenation Cracking Unit. The risk level (low, medium, medium-high, and high) of 553 equipment and/or piping items of the systems that compose the unit was obtained.

Ahmadi and Kumar (2011) proposed a cost rate function (CRF) to identify inspection and restoration intervals of hidden failures (while the system is in a non-operating state) for repairable components. The proposed method considers the costs associated with inspection, repair/restoration and failure. The optimum inspection interval is obtained at the minimum value of the CRF.

## 1.7. Thesis overview

The organizational structure of the entire thesis is given in Figure 1-3 and the overview of each chapter is discussed below:

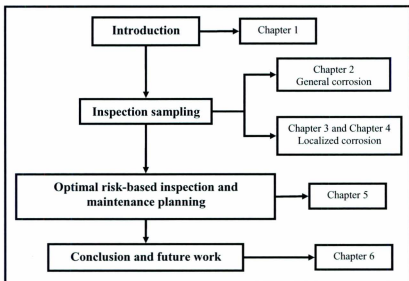


**Figure 1-3:** Thesis organization.

Chapter 1 provides an overview of inspection and maintenance planning approaches. This chapter also discusses risk-based inspection and maintenance approach focusing on process assets.

Chapter 2 introduces a Bayesian approach to estimate sample size for inspection of general corrosion of process components.

Chapter 3 introduces a methodology to calculate sample size in order to assess localized corrosion of process components. This chapter highlights the steps of the methodology and its use of the extreme value and bootstrap methods.

Chapter 4 discusses an algorithm that integrates the extreme value method and Bayesian updating approach to estimate sample size. The objective of this algorithm is to assess localized corrosion in process components.

Chapter 5 introduces a methodology for optimal risk-based inspection and maintenance planning for process systems. This chapter highlights optimal selection of inspection interval, inspection technique and maintenance activity based on minimizing the inspection and maintenance cost without compromiozing the safety.

Chapter 5 highlights the conclusion and future work. Also, this chapter discusses the significance and originality of the thesis.

## **CHAPTER 2**

### **Inspection Sampling of General Corrosion- A Bayesian Approach<sup>1</sup>**

#### **Abstract**

A Bayesian approach-based method is proposed for calculating the minimum size of a sample to assess, with a specified precision, the integrity of process assets suffering from general corrosion. The proposed method ensures that the error in the posterior estimate of the mean does not exceed a pre-defined acceptable margin of error at a specified confidence level. The sample size obtained using the proposed method is smaller than a sample size obtained using the classical method with same confidence level. This reduces sampling inspection cost without affecting the precision of the estimate.

---

<sup>1</sup> Part of this chapter has been published in a peer-reviewed journal “Khalifa, M., Khan, F. and Haddara, M. (2012). Bayesian sample size determination for inspection of general corrosion of process components. Journal of Loss Prevention in the Process Industries, 25, 218-223”. To minimize repetition, the related references are listed in the thesis reference list.

## **2.1. Introduction**

In engineering applications, decisions are often made based on whatever limited available information. The information that is available before performing a new inspection is referred to as prior (past) information. This information can be based on historical data, theoretical models or subjective judgement. One can use newly obtained inspection data to update prior information using Bayesian updating theory. The updated information is referred to as posterior information. For example, prior information of metal loss of equipment can be updated once a new set of inspection data is obtained. Although the choice of a prior is often subjective, a rational agreement can be achieved by analyzing historical data obtained from the same or similar piece of equipment. Details of statistical methods used to estimate priors are presented by Thodi, et al. (2009).

The difference between a Bayesian approach-based method and the classical method for sample size determination is that a Bayesian approach-based method combines prior (past) information with the observed data. In the classical method, sample size is estimated based on newly observed data or prior information. There is no formal basis to combine past and newly observed data for estimating sample size in the classical method (Ang and Tang, 2007).

The objective of this chapter is to develop a Bayesian approach-based method for the determination of the minimum sample size needed to assess the mean metal loss of process components due to general corrosion.

## **2.2. The classical method for sample size calculation**

According to the central limit theorem, the probability distribution of the mean of all possible samples of size  $n$ , taken from a population having a mean of,  $\mu$ , and a standard deviation,  $\sigma$ , is approximately normal. The resulting normal distribution is called the sampling distribution of the sample mean. This distribution has a mean and standard deviation equal to  $\mu$  and  $\sigma/\sqrt{n}$ , respectively, provided that the sample size,  $n$ , is sufficiently large. This approximation improves as the value of  $n$  increases. There is no exact rule to determine the appropriate value of  $n$  which satisfies the condition “sufficiently large” given in the central limit theorem. The sample size  $n$  that is required for applying the central limit theorem varies as a function of the shape of the population distribution. The closer the population’s distribution to the normal, the smaller the sample size needed. It has been stated that a sample of size,  $n = 20$ , is appropriate for populations having normal distributions, while a size of  $n = 30$ , is appropriate for populations skewed from the normal distribution (Bernstein and Bernstein, 1999).

The margin of error of the mean,  $MOE_{mean}$ , is the deviation between the population mean,  $\mu$ , and the sample mean,  $\mu_s$ , it is given by:

$$MOE_{mean} = | \mu - \mu_s | \quad (2.1)$$

The margin of error is a measure of the adequacy of the sample to be used to describe the population. An adequate sample size ensures that the margin of error does not exceed a predefined acceptable value, with a specified confidence level of  $(1-\alpha)$ . The confidence level of a margin of error indicates the likelihood that the difference between the population value and the sample estimate is less than or equal to this margin of error.

$MOE_{mean}$  is expressed as half the width of the confidence interval  $(1-\alpha)$  for the sampling distribution of the mean (i.e., the distribution of the sample mean) as follows:

$$MOE_{mean} = \Phi^{-1}(1-\alpha/2) \cdot \frac{\sigma}{\sqrt{n}} \quad (2.2)$$

where  $\sigma$  is the standard deviation of the population,  $\Phi^{-1}$  is the inverse standard normal probability, and  $\alpha$  is significance level.  $(\sigma/\sqrt{n})$  is the standard deviation of the sampling distribution of the mean (i.e., standard deviation of the sample mean,  $\mu_s$ ).

The required sample size,  $n$ , to evaluate the mean of infinite population is obtained from Eq. 2.2 as follows:

$$n = [\Phi^{-1}(1-\alpha/2) \cdot \sigma / \text{MOE}_{\text{mean}}]^2 \quad (2.3)$$

One can use a t-distribution when the population's standard deviation,  $\sigma$ , is unknown and has to be estimated from the data. In this case,  $\Phi^{-1}(1-\alpha/2)$  and  $\sigma$  used in Eq. 2.3 are replaced with  $t_{1-\alpha/2,n-1}$  and the sample standard deviation,  $\sigma_s$ , respectively as follows:

$$n = [t_{1-\alpha/2,n-1} \cdot \sigma_s / \text{MOE}_{\text{mean}}]^2 \quad (2.4)$$

where  $t_{1-\alpha/2,n-1}$  is the upper critical value at the probability of  $(1-\alpha/2)$  of the t-distribution with  $(n-1)$  degree of freedom.

Eqs. 2.3 and 2.4 are used when the population size ( $N$ ) is infinite or practically large in comparison to the sample size,  $n$ . If the population is finite, the standard deviation is multiplied by a finite population correction factor (FPCF) given by (Bernstein and Bernstein, 1999):

$$\text{FPCF} = \sqrt{(N-n)/(N-1)} \quad (2.5)$$

Since the population size,  $N$  is usually much larger than 1, the FPCF can be approximated as:

$$FPCF \approx \sqrt{1 - n/N} \quad (2.6)$$

When the ratio  $n/N$  is less than 0.05, the correction factor has small effect and the population may be considered practically infinite.

Using Eq. 2.6 and Eq. 2.3, a classical formula to calculate the required sample size  $n$  to evaluate the mean of a population of size  $N$  with pre-defined acceptable margin of error ( $MOE_{accept}$ ) is given by, see ASTM E122 (2009):

$$n = \frac{\left[ \Phi^{-1}\left(1 - \frac{\alpha}{2}\right) \left( \frac{\sigma}{MOE_{accept}} \right) \right]^2}{1 + \frac{\left[ \Phi^{-1}\left(1 - \frac{\alpha}{2}\right) \left( \frac{\sigma}{MOE_{accept}} \right) \right]^2}{N}} \quad (2.7)$$

### 2.3. A proposed Bayesian approach-based method of sample size calculation

#### 2.3.1. Posterior estimate of sample mean and standard deviation

Let  $x$  denotes observed independent sample data. Assume the distribution of the random variable,  $x$ , has a parameter  $\theta$ . Assume further, that the parameter  $\theta$  is

a random variable having a known prior probability distribution  $f(\theta)$ . The prior distribution of the parameter  $\theta$  can be updated using Bayes' theorem as follows:

$$f''(\theta) = \frac{P(x|\theta) f(\theta)}{\int_{-\infty}^{\infty} P(x|\theta) f(\theta) d\theta} \quad (2.8)$$

where  $f''(\theta)$  is the posterior (updated) probability distribution of  $\theta$  and  $P(x|\theta)$  is the conditional probability of observing the inspection outcome  $x$  for a given  $\theta$  and commonly referred to as the likelihood function of  $\theta$ .

The posterior estimate,  $\theta''$ , for the mean of the parameter  $\theta$  is given by:

$$\theta'' = \int_{-\infty}^{\infty} \theta f''(\theta) d\theta \quad (2.9)$$

Let the parameter  $\theta$  denotes the mean of the corrosion depth and assume that it is normally distributed. Further assume that the prior distribution of the mean is normal. In this case, the posterior distribution of the sample mean is also normal. The posterior estimate for the mean and the standard deviation of the sample mean are obtained from Bayes' theorem as follows (Ang and Tang, 2007):

$$\mu''_{\mu s} = \frac{\mu_x (\sigma'_{\mu s})^2 + \mu' \cdot \left( \frac{\sigma_x^2}{n} \right)}{(\sigma'_{\mu s})^2 + \left( \frac{\sigma_x^2}{n} \right)} \quad (2.10)$$

$$\sigma''_{\mu s} = \sqrt{\frac{(\sigma'_{\mu s})^2 \cdot (\frac{\sigma_s^2}{n})}{(\sigma'_{\mu s})^2 + (\frac{\sigma_s^2}{n})}} \quad (2.11)$$

where  $\sigma'_{\mu s}$  is the prior estimate of the standard deviation of the sample mean and  $\sigma_s$  is the standard deviation of the sample of size n.  $\mu'$  is the prior mean.

If all possible random samples, each of size n, are drawn from a prior distribution with standard deviation of  $\sigma'$  and the mean of each sample is estimated, the prior standard deviation of the sample mean,  $\sigma'_{\mu s}$ , is given by:

$$\sigma'_{\mu s} = \sigma'/\sqrt{n} \quad (2.12)$$

Substituting for  $\sigma'_{\mu s}$  in Eq. 2.10 and Eq. 2.11, one gets:

$$\mu''_{\mu s} = \frac{\mu_p \sigma'^2 + \mu' \sigma_s^2}{\sigma'^2 + \sigma_s^2} \quad (2.13)$$

$$\sigma''_{\mu s} = \sqrt{\frac{\left(\frac{\sigma'^2}{n}\right) \cdot \left(\frac{\sigma_s^2}{n}\right)}{\left(\frac{\sigma'^2}{n}\right) + \left(\frac{\sigma_s^2}{n}\right)}} \quad (2.14)$$

$$\sigma''_{\mu s} = \sqrt{\frac{\sigma'^2 \sigma_s^2}{\sigma'^2 + \sigma_s^2}} / \sqrt{n} \quad (2.15)$$

$$\sigma''_{\mu s} = \sigma^*/\sqrt{n} \quad (2.16)$$

$$\text{where } \sigma^* = \sqrt{\frac{\sigma_r^2 \cdot \sigma_s^2}{\sigma_r^2 + \sigma_s^2}}$$

Eqs. 2.13 and 2.16 give expressions for the posterior estimates of the sample mean and standard deviation in terms of the new and prior information.

When prior information and new sample inspection data are available, the population's properties can be estimated on the basis of the posterior estimates for the parameters. For uninformative prior information (i.e.,  $\sigma^*$  approaches infinity),

from Eqs. 2-13 and 2-14, the limit of  $\mu''_{\mu s}$  approaches the sample mean,  $\mu_s$  and the limit of  $\sigma''_{\mu s}$  approaches  $\sigma_s/\sqrt{n}$  as in the classical method.

### 2.3.2. Calculation of the sample size

For a finite population,  $\sigma''_{\mu s}$  is obtained using Eq. 2.6 and Eq. 2.16 as follows:

$$\sigma''_{\mu s} = \frac{\sigma^*}{\sqrt{n}} \cdot \sqrt{1 - \frac{n}{N}} \quad (2.17)$$

$$\sigma''_{\mu s} = \sigma^* \cdot \sqrt{\frac{1}{n} - \frac{1}{N}} \quad (2.18)$$

The margin of error of the posterior sample mean can be defined by replacing the standard deviation of the sample mean ( $\sigma/\sqrt{n}$ ) in the classical method (Eq. 2.1) with the posterior standard deviation of the sample mean ( $\sigma''_{\mu s}$ ).

$$MOE_{mean} = \Phi^{-1}(1 - \alpha/2) \cdot \sigma''_{\mu s} \quad (2.19)$$

Using Eqs 2.18 and 2.19, a formula to estimate the required sample size n to evaluate the posterior mean of a population of size N with pre-defined acceptable margin of error (MOE<sub>accept</sub>) can be obtained as

$$n = \frac{\left[ \Phi^{-1}\left(1 - \frac{\alpha}{2}\right) \cdot \left( \frac{\sigma^*}{MOE_{accept}} \right) \right]^2}{1 + \frac{\left[ \Phi^{-1}\left(1 - \frac{\alpha}{2}\right) \cdot \left( \frac{\sigma^*}{MOE_{accept}} \right) \right]^2}{N}} \quad (2.20)$$

$$\text{where } \sigma^* = \sqrt{\frac{\sigma_r^2 \cdot \sigma_s^2}{\sigma_r^2 + \sigma_s^2}}$$

Eq. 2.20 can be solved using an iterative scheme. First a sample size is assumed and inspection data is obtained for this sample. The standard deviation,  $\sigma_s$ , is estimated from the sample data. If the sample size, n, and the estimated

sample standard deviation,  $\sigma_s$ , satisfy Eq. 2.20, then the iterations process is stopped.

The proposed formula (Eq. 2.20) is similar to the classical formula (Eq. 2.7) except that the population standard deviation,  $\sigma$ , is replaced with  $\sigma''$ . It may be noticed that the estimated sample size from the proposed formula is always less than the estimated sample size using the classical formula. This fact can be proved mathematically as follows:

The expression of  $\sigma''$  in Eq. 2.20 can be re-written as:

$$\sigma'' = \sqrt{\frac{\sigma'^2 \cdot \sigma_s^2}{\sigma'^2 + \sigma_s^2}} = \sigma' \cdot \sqrt{\frac{\sigma_s^2}{\sigma'^2 + \sigma_s^2}} = \sigma_s \cdot \sqrt{\frac{\sigma'^2}{\sigma'^2 + \sigma_s^2}}$$

This expression shows that  $\sigma''$  is equal to  $\sigma'$  or  $\sigma_s$  multiplied by a coefficient of a magnitude  $< 1$ . It is clear that  $\sigma''$  is less than both the prior standard deviation  $\sigma'$  and the sample standard deviation  $\sigma_s$ . The population standard deviation,  $\sigma$ , in the classical formula is assumed to be equal to  $\sigma'$  or  $\sigma_s$ . Therefore, the estimated sample using the proposed formula is always less than the estimated sample size using the classical formula. This allows the use of a sample having a smaller size to get results having the same level of precision (i.e.,  $MOE_{accept}$ ) with the same confidence level ( $1-\alpha$ ).

## 2.4. Case study

Assume that a population of size  $N = 100$  components is subjected to general corrosion. Further, assume that the prior distribution of the corrosion depth is normal with mean,  $\mu'$ , and standard deviation,  $\sigma'$ , of 5 mm and 0.7 mm, respectively. It is required to estimate sample size to assess the mean corrosion depth of this population with  $MOE_{accept}$  of 0.1 mm at confidence level  $(1-\alpha)$  of 95%.

Classical method (Eq. 2.7):

$$n = \frac{\left[ \Phi^{-1}(1-\frac{\alpha}{2}) \left( \frac{\sigma}{MOE_{accept}} \right) \right]^2}{1 + \frac{\left[ \Phi^{-1}(1-\frac{\alpha}{2}) \left( \frac{\sigma}{MOE_{accept}} \right) \right]^2}{N}}$$

The standard deviation in Eq. 2.7 is assumed known and equal to the prior standard deviation,  $\sigma' = 0.7$  mm.

$$n = \frac{\left[ 1.96 * \left( \frac{0.7}{0.1} \right) \right]^2}{1 + \frac{\left[ 1.96 * \left( \frac{0.7}{0.1} \right) \right]^2}{100}}$$

$$n = 66$$

Proposed method (Eq. 2.20):

$$n = \frac{\left[ \Phi^{-1} \left( 1 - \frac{\alpha}{2} \right) \cdot \left( \frac{\sigma''}{\text{MOE}_{\text{accept}}} \right) \right]^2}{1 + \frac{\left[ \Phi^{-1} \left( 1 - \frac{\alpha}{2} \right) \cdot \left( \frac{\sigma''}{\text{MOE}_{\text{accept}}} \right) \right]^2}{N}}$$

$$\text{where } \sigma'' = \sqrt{\frac{\sigma_s^2 \cdot \sigma_a^2}{\sigma_s^2 + \sigma_a^2}}$$

Using iterative process in the above equation, a sample size of 50 was estimated. Table 2-1 shows the sample data (corrosion depth of 50 components) with  $\mu_s = 5.13$  mm and  $\sigma_s = 0.71$ mm.

**Table 2-1:** Sample data ( $n=50$ ) in mm for population size N=100.

3.3	4.5	4.7	4.4	5.1
4.6	5.2	5.1	4.5	6.5
4.7	4.9	5.6	5.2	5.2
5.9	5.8	5.7	6.5	6.4
5.1	5.8	5.3	4.1	4.6
4.8	6.1	4.8	4.3	5.1
6.2	4.5	4.7	5.1	4.6
4.9	5.8	6.0	5.1	5.1
4.8	4.2	5.9	4.3	6.4
5.3	5.5	5.4	3.9	4.9

The data shown in Table 2-1 was randomly selected from a population generated with Monte Carlo simulation while in real applications it should be obtained from inspection of randomly selected components/areas. The generated population represents the actual population. The sample size (50) obtained in this

example using the proposed method is 25% less than the sample size (66) obtained using the classical method with the same precision and same confidence level.

Figure 2-1 shows normal probability plot of sample data in Table 2-1 indicating a good fit to normal distribution.

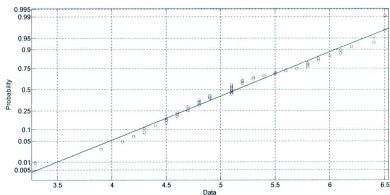


Figure 2-1: Normal probability plot of sample data shown in Table 2-1.

The posterior sample mean is estimated from Eq. 2.13 as follows:

$$\mu_{\text{us}}'' = \frac{\mu_s \cdot \sigma'^2 + \mu' \cdot \sigma_s^2}{\sigma'^2 + \sigma_s^2}$$

$$\mu_{\text{us}}'' = \frac{5.13 * 0.7^2 + 5 * 0.71^2}{0.7^2 + 0.71^2}$$

$$\mu''_{\mu s} = 5.1 \text{ mm}$$

The margin of error in this estimate is 0.1 mm at the specified confidence level (95%).

Effect of prior information on sample size:

It is given in this case study that the prior mean,  $\mu'$ , and standard deviation,  $\sigma'$ , are 5 mm and 0.7 mm, respectively.

Assuming same prior mean,  $\mu' = 5$  mm, sample mean  $\mu_s = 5.13$  mm, sample standard deviation,  $\sigma_s = 0.71$  mm and population size,  $N = 100$  but different values of the prior standard deviation,  $\sigma'$ . Sample size is estimated using Eq. 2.20 and posterior sample mean is estimated using Eq. 2.13 as shown in Table 2-2.

**Table 2-2:** Sample size and posterior sample mean for different prior standard deviations.

prior standard deviation, $\sigma'$ , mm	Sample size, n	Posterior sample mean, $\mu_{\mu_s}$ , mm
0.3	23	5.02
0.7	50	5.06
1	57	5.09
10	65	5.13
Infinity	66	5

From Table 2-2, it is observed that sample size increases with the increase in prior standard deviation and finally approaches the sample size estimated using the classical method when prior standard deviation approaches infinity (uninformative prior). The posterior sample mean falls between the sample mean ( $\mu_s = 5$  mm) and the prior mean ( $\mu' = 5.13$  mm) weighted by the variance as shown in Eq. 2.13. When prior standard deviation approaches infinity (uninformative prior), the posterior sample mean approaches sample mean,  $\mu_s$ . In this case of uninformative prior, the proposed method yields to the classical method.

Assuming same prior standard deviation,  $\sigma' = 0.7$  mm, sample mean,  $\mu_s = 5.13$  mm, sample standard deviation,  $\sigma_s = 0.71$  mm and population size,  $N = 100$  but different values of the prior mean,  $\mu'$ . Sample size and posterior mean are shown in Table 2-3.

**Table 2-3:** Sample size and posterior mean for different values of prior mean.

prior mean, $\mu'$ , mm	Sample size, n	Posterior sample mean, $\mu_{\mu^*}$ , mm
3	50	4
5	50	5.1
7	50	6.1
10	50	7.6
20	50	12.7

From Table 2-3, the prior mean does not affect the sample size however affects the posterior sample mean which is considered to evaluate the population mean. The classical method does not account for the prior mean in evaluating the population mean.

#### Effect of the population size on sample size

Various population sizes are considered to estimate sample size using the proposed and classical method. Table 2-4 shows the results of sample size and the saving in sample size compared to the classical method.

**Table 2-4:** Sample size for different population size, N.

Population size, N	Prior standard deviation, $\sigma'$ , (mm)	Sample standard deviation, $\sigma_s$ , (mm)	Table of sample data	Sample size, n		Saving %
				Classical formula (Eq. 2.7)	Proposed formula (Eq. 2.20)	
50	0.7	0.77	2-5	40	33	18
100	0.7	0.71	2-1	65	49	25
200	0.7	0.78	2-6	97	65	33
1000	0.7	0.68	2-7	158	88	44

Tables 2-5, 2-6 and 2-7 show sample data for population size N= 50, 200 and 1000 respectively.

**Table 2-5:** Sample data (33 data points in mm) for population size N=50.

4.8	5.3	5.2	4.5	4.7
5.3	4.6	5.1	5.5	3.8
5.1	5.3	5.0	6.7	4.3
4.9	6.3	4.4	5.3	5.0
4.0	4.0	5.2	4.8	5.2
4.5	6.3	3.6	4.0	4.4
6.6	3.5	4.5		

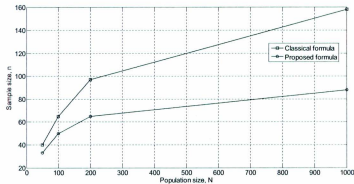
**Table 2-6:** Sample data ( $n = 65$ ) in mm for population size  $N=200$ .

6.1	5.2	5.2	4.8	5.2
4.5	5.5	4.8	5.6	5.2
5.2	4.3	6.4	3.7	4.8
5.3	4.6	4.6	5.1	5.3
5.3	4.3	4.5	5.0	5.5
5.0	5.5	4.6	6.0	7.1
4.9	4.6	4.8	4.3	5.0
5.3	4.9	5.8	4.4	5.3
4.8	5.0	6.9	6.4	6.0
4.4	4.8	5.1	2.6	4.6
4.1	4.5	5.4	6.4	4.7
4.9	4.8	3.6	5.5	4.6
4.9	5.5	5.2	4.7	4.1

**Table 2-7:** Sample data (88 data points in mm) for population size  $N=1000$ .

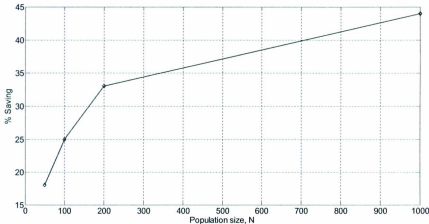
5.3	5.2	5.0	5.5	4.8
4.8	5.0	4.6	5.9	4.5
4.7	5.1	4.7	4.1	4.3
4.8	4.9	5.4	4.2	5.9
5.6	5.7	4.6	4.9	5.6
4.8	3.7	6.1	4.6	4.6
5.1	4.4	3.9	4.4	6.6
4.9	4.4	5.4	5.2	4.3
6.4	5.4	5.5	4.8	5.2
5.4	4.6	4.2	5.0	4.8
4.2	3.8	4.4	4.5	6.1
5.2	6.5	5.4	5.8	5.3
3.8	4.6	5.1	5.8	5.3
5.3	4.3	5.1	4.5	6.1
5.4	4.1	4.0	4.0	3.5
4.6	5.4	5.5	4.1	3.8
4.4	4.2	4.4	5.4	4.6
3.9	5.6	4.5		

Figure 2-2 shows sample size,  $n$ , for different population size,  $N$ . The sample size estimated using the proposed method is less than the classical method. This allows using a smaller sample size with the same precision.



**Figure 2-2:** Sample size,  $n$ , for different population size,  $N$ .

Figure 2-3 shows the percentage of saving in sample size when using the proposed method compared to the classical method for different population size,  $N$ . The larger the population size, the more saving in inspection sample and therefore saving in sampling inspection cost.



**Figure 2-3:** Percentage of saving when using the proposed formula in comparison to the classical formula for different population size,  $N$ .

## 2.5. Conclusion

A Bayesian approach-based method is proposed to determine the minimum size of inspection samples required to assess the condition of process components subjected to general corrosion. The population mean metal loss due to general corrosion is evaluated based on the posterior sample mean. The sample size is estimated to guarantee an acceptable margin of error in the estimate of the posterior sample mean at a given confidence level. The proposed method uses current inspection data to update prior information using a Bayesian updating process.

A closed form formula is proposed to estimate sample size for evaluation of the mean metal loss for a finite population subjected to general corrosion. The proposed formula is a function of the sample standard deviation, prior standard deviation of the metal loss, population size, the acceptable margin of error and the specified confidence level. The estimated sample size ensures that the error in the posterior estimate of the mean metal loss due to general corrosion does not exceed a pre-defined acceptable margin of error at a specified confidence level.

The suggested method was tested on a case study which showed that the sample size obtained using the proposed method is smaller than the sample size obtained using the classical method for the same confidence level. For example, the percentage of reduction in sample size is 25% for a population size of 100 and 44% for a population size of 1000 for the same confidence level of 95%.

## **CHAPTER 3**

### **Inspection Sampling of Localized Corrosion- A Statistical Approach<sup>2</sup>**

#### **Abstract**

A methodology to estimate the required sample size to assess, with a specified precision, the localized corrosion of process assets has been proposed. The proposed methodology uses the extreme value and bootstrap statistical methods. The estimated sample size ensures that the predicted maximum localized corrosion, with the extreme value method, is within an acceptable margin of error at a specified confidence level. Using the results of the proposed methodology, an equation is introduced to calculate sample size as a function of the acceptable margin of error, the population size, the standard deviation of corrosion data and the required confidence level. The methodology is explained through a case study of localized corrosion in process piping.

---

<sup>2</sup> Part of this chapter has been published in a peer-reviewed journal "Khalifa, M., Khan, F. and Haddara, M. (2012). A Methodology For Calculating Sample Size To Assess Localized Corrosion of Process Components. Journal of Loss Prevention in the Process Industries, 25, 70-80". To minimize repetition, the related references are listed in the thesis reference list.

### **3.1. Introduction**

This chapter proposes a methodology to estimate the required sample size to assess, with a specified precision, the localized corrosion of process assets.

The extreme value method is widely used to predict the maximum localized corrosion over the entire population using sample data. The sample data represent the maximum corrosion size in each inspected component/area. A major limitation of the application of the extreme value method to the assessment of the localized corrosion is that the sample size affects the accuracy of the extreme value prediction (Jarrah et al., 2011). The proposed methodology calculates the sample size to assess, with a specified precision, the maximum localized corrosion of process components. The precision is quantified by a margin of error (MOE) of the predicted maximum corrosion over the entire asset/system. This MOE is estimated using the finite population bootstrap method. The estimated MOE is compared to the acceptable margin of error to determine the minimum required sample size.

### **3.2. Proposed methodology to estimate sample size for the inspection of localized corrosion**

The proposed methodology compromises the following main parts as shown on the methodology flowchart (Figure 3-1):

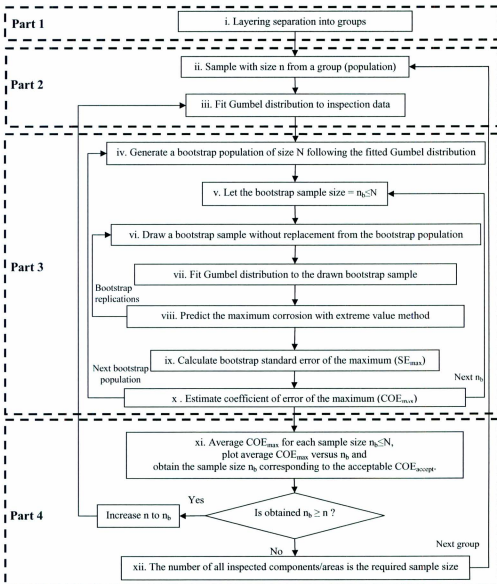


Figure 3-1: Proposed methodology flowchart.

### **3.2.1. Part 1- Layering separation**

Through layering separation the equipment of an installation subjected to corrosion are classified into groups or areas. The groups obtained by this classification process are usually referred to as corrosion circuits or loops. A corrosion circuit (loop) is a group of similar assets in the plant which have the same material and exposed to the same corrosion conditions. Each group is considered as a population from which sampling is required. The objective of layering separation is to reduce the source of variability in the inspection data within each group. This would help to reduce the required sample size when sampling randomly within a group because sample size is strongly dependent on the standard deviation,  $\sigma$ , of the population.

### **3.2.2. Part 2- Physical sampling within each group**

A randomly selected number of components/areas within a group is inspected. Only the maximum localized corrosion of each component/area is recorded and fitted to a Gumbel extreme value distribution.

### 3.2.3. Part 3- Bootstrap sampling and extreme value analysis

#### 3.2.3.I. Use of bootstrap sampling methods to estimate standard error and confidence interval

The standard error of an estimator is a measure of the accuracy of an estimator obtained based on sample data. There is no accurate formula for estimating the standard error of a statistic other than the mean.

The standard error of the mean,  $SE_{mean}$  is given by:

$$SE_{mean} = \frac{\sigma}{\sqrt{n}} \quad (3.1)$$

where  $\sigma$  is the standard deviation of the population and  $n$  is the sample size.

The confidence interval, CI, is estimated as a multiple of the standard error, SE, as follows:

$$CI = 2 \cdot \Phi^{-1} \left( 1 - \frac{\alpha}{2} \right) \cdot SE \quad (3.2)$$

where  $\Phi^{-1}$  is the inverse of the standard normal distribution and  $(1-\alpha)$  is the confidence level.

The margin of error of an estimator obtained using sample data is the maximum acceptable deviation of this estimator from the actual value. It expresses the required estimate precision. For example, if the desired precision is set at  $\pm 0.1$  mm, then the margin of error is 0.1 mm.

The margin of error is expressed as half the width of the confidence interval. From Eqs. 3.1 and 3.2, the margin of error of the mean,  $MOE_{mean}$ , is given by:

$$MOE_{mean} = \Phi^{-1}(1 - \alpha/2) \cdot \frac{\sigma}{\sqrt{n}} \quad (3.3)$$

In case of localized corrosion, as there is no closed-form analytical expression to estimate the confidence interval and therefore the margin of error of the maximum localized corrosion, bootstrap sampling is used in the proposed methodology for this purpose. Bootstrap sampling is a simulation of physical sampling process. It is a convenient tool that requires less assumptions and computations.

In bootstrapping, a resample called bootstrap sample can be drawn randomly with one of three main procedures:

- i. From the sample data itself (with replacement). This procedure is referred to as non-parametric bootstrap and was first proposed by

Efron (1979) to estimate the standard error and confidence interval when the standard methods cannot be used.

- ii. From a created virtual population (either with or without replacement). This population is called bootstrap population. An example of this procedure is the finite population bootstrap (FPB) which was first introduced by Gross (1980). The simplest case when the population size,  $N$ , is a multiple of the sample size,  $n$  (i.e.,  $N=C.n$ ). In this case the bootstrap population is created by repeating the sample  $C$  times (Cohen, 1997). In real sampling applications, the sample is taken from a finite population without replacement. Thus, in the proposed methodology, the FPB method without replacement is used. The bootstrap population is generated using Monte Carlo simulation following Gumbel extreme value distribution of the sample data.
- iii. From a distribution fits the sample data assuming that the sample distribution is an approximation to the population distribution. This maybe called a Monte Carlo procedure (Brooker, D.C. and Geoffery K.C., 2004) and also referred to parametric bootstrap. This procedure is useful where a parametric model fits the population distribution is

known. It is more accurate than non-parametric bootstrap (Efron and Tibshirani, 1993).

The steps of bootstrapping to estimate standard error and confidence intervals are summarized as follows:

I. Bootstrap sample:

Draw a bootstrap sample.

II. Bootstrap statistic:

A statistic such as mean, median or maximum is evaluated for large number of bootstrap samples.

III. Bootstrap distribution:

Bootstrap distribution of bootstrap statistic is obtained.

IV. Bootstrap standard error and confidence interval:

The standard error and confidence interval of the statistic are estimated as the standard deviation and confidence interval for the mean of the bootstrap distribution, respectively.

Figure 3-2 shows a flowchart of bootstrapping to estimate standard error and confidence intervals.

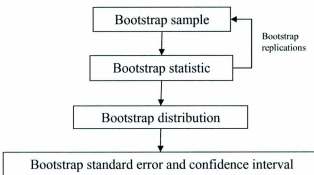


**Figure 3-2:** Bootstrapping to estimate standard error and confidence intervals.

In the proposed methodology, a large number of bootstrap samples of different sizes  $n_b \leq N$  are drawn without replacement from generated bootstrap populations of the same size of the original population,  $N$ . The maximum localized corrosion is predicted with the extreme value method for each bootstrap sample. The bootstrap standard error of the maximum corrosion,  $SE_{max}$ , predicted with the extreme value method is estimated.

### *3.2.3.2. Use of the extreme value statistical method to predict the maximum localized corrosion*

The extreme value distribution is classified into three types (Type I, Type II and Type III) for two cases (maximum values and minimum values). Type I (in case of maximum values) is known as Gumbel distribution. As the objective of inspection in case of localized corrosion is to evaluate the maximum localized

corrosion size, it is a common practice to use the extreme value distribution (type I) to represent the probability distribution of maximum localized corrosion; see Kowako et al. (1984).

The inspection data modeled by extreme value distribution (case of maximum values) may be extrapolated for the whole population to predict the maximum corrosion size in uninspected areas (Kowaka et al., 1984); The Health and Safety Executive, 2002; and ASTM G46-94, 2005).

The cumulative probability of Gumbel distribution of the maximum corrosion size in each component/area,  $x$ , is given by:

$$F(x) = \text{Exp} \left( -\text{Exp} \left( -\frac{x-\lambda}{\theta} \right) \right) \quad (3.4)$$

where  $\lambda$  and  $\theta$  are location and scale parameters, respectively.

The mean,  $\mu$  and standard deviation,  $\sigma$  are estimated in terms of  $\lambda$  and  $\theta$  as follows:

$$\mu = \lambda + \gamma\theta \quad (3.5)$$

where  $\gamma = 0.57722$  is Euler constant.

$$\sigma = \frac{\pi}{\sqrt{6}} \theta \quad (3.6)$$

To demonstrate how the maximum corrosion is predicted over the whole population with the extreme value method, let us consider a system having a total of  $N$  components/areas (population of size  $N$ ) and a sample of size  $n$  components/areas is inspected. The sample data points (measured maximum corrosion for each component/area) are arranged in order of increasing rank. The cumulative probability,  $F$ , can be calculated as  $i/(n+1)$ , when using the average rank method, where  $i$  is the order of rank and  $n$  is the sample size (number of recorded maxima). The highest value of the sample cumulative probability can be estimated as  $F=n/(n+1)$ . This maximum value corresponds to the maximum corrosion over the sample. Similarly, the highest value of the cumulative probability for the whole population of size  $N$  can be estimated as  $F_{max}=N/(N+1)$ . The Gumbel probability plot is obtained by plotting  $-\ln(-\ln(F(x)))$  versus  $x$ . The maximum corrosion size,  $x_{max}$ , over a population of size  $N$  using sample data of size  $n$  is obtained by extrapolation of the fitted straight line in Gumbel probability plot from point A to point B as shown in Figure 3-3.

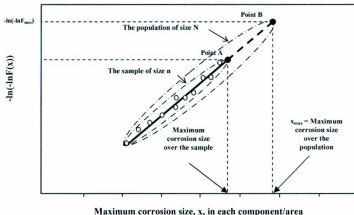


**Figure 3-3:** Extrapolation of Gumbel probability plot to predict the maximum localized corrosion over the entire population.

Point A corresponds to the maximum corrosion size over the sample of size  $n$ . Point B corresponds to the maximum corrosion size over the entire population of size  $N$  assuming the sample represents the population. The plotting position of point A on the vertical axis is the maximum cumulative probability of the maximum corrosion size in each component/area of the sample. The plotting position of point B on the vertical axis is  $-\ln(-\ln F_{\max})$ .

The predicted maximum value using the extrapolation shown in Figure 3-3 is affected by sample size. Thus, determining sample size is important to ensure the precision of the extreme value prediction of the maximum corrosion.

### 3.2.4. Part 4- Calculation of the required sample size to predict the maximum localized corrosion within each group

It is required to estimate the appropriate sample size within each group which provides an accurate description of the state of the whole group.

When the sampling objective is to evaluate the population mean, the sample size is estimated as follows:

- a) When the standard deviation of the population,  $\sigma$ , is known, Eq. 3.3 leads to a sample size  $n$ , corresponding to a pre-defined acceptable margin of error,  $MOE_{accept}$ , given by:

$$n = \left[ \phi^{-1} \left( 1 - \frac{\alpha}{2} \right) \cdot \left( \frac{\sigma}{MOE_{accept}} \right) \right]^2 \quad (3.11)$$

- b) When the standard deviation of the population,  $\sigma$ , is unknown and has to be estimated from the data, one can use t-distribution. In this case,  $\Phi^{-1} \left( 1 - \frac{\alpha}{2} \right)$  and  $\sigma$  used in Eq. 3-11 are replaced with  $t_{1-\alpha/2,n-1}$  and  $\sigma_s$ , respectively as follows:

$$n = \left[ t_{1-\frac{\alpha}{2},n-1} \cdot \left( \frac{\sigma_s}{MOE_{accept}} \right) \right]^2 \quad (3.12)$$

where  $t_{1-\alpha/2,n-1}$  is the critical value at the probability of  $(1-\alpha/2)$  of the t-distribution with  $(n-1)$  degree of freedom and  $\sigma_s$  is the sample standard

deviation. For large sample size  $n$  (for example  $n > 50$ ), the t-distribution approaches the standard normal distribution. In this case, the above two equations give approximately equal sample sizes. The solution for  $n$  in Eq. 3.12 should be obtained by trial and error because  $t_{1-\alpha/2,n-1}$  is a function of  $n$ .

- c) If the population is finite, the standard deviation in Eqs. 3.11 and 3.12 is multiplied by a finite population correction factor (FPCF) is given by Eqs. 2.5 and 2.6. Instead of multiplying the standard deviation by FPCF, the sample size obtained from Eq. 3.11 is divided by  $(1+n/N)$  as suggested by ASTM E122 (2009). This yields to the following classical equation for calculating the sample size needed for the evaluation of the mean of a finite population:

$$n = \frac{\left[ \frac{t_{1-\alpha/2}^2}{2} \left( \frac{\sigma}{MOR_{accept}} \right)^2 \right]^2}{1 + \left[ \frac{t_{1-\alpha/2}^2}{2} \left( \frac{\sigma}{MOR_{accept}} \right)^2 \right] \frac{N}{N}}$$
(3.13)

In case of localized corrosion, evaluation of the mean is not sufficient because the failure is expected when the maximum corrosion at any location in the population exceeds the critical limit. Thus, the sampling objective is to predict the maximum corrosion, not the mean, over the whole population (inspected and uninspected components/areas). In order to achieve that, the following steps are undertaken in the proposed methodology:

- I. Standard error of the population maximum ( $SE_{max}$ ) is estimated as the standard deviation of the population maximum which is predicted using the extreme value method for large number of bootstrap samples of sizes  $n_b \leq N$  (see Figures 3.2 and 3.3).
- II. The ratio of standard error of the population maximum ( $SE_{max}$ ) to standard deviation of sample data ( $\sigma_s$ ) is evaluated for each bootstrap sample. In this work, we will refer to this ratio as the coefficient of error of the population maximum ( $COE_{max}$ ) and define it as follows:

$$COE_{max} = SE_{max}/\sigma_s \quad (3.14)$$

The coefficient of error is dimensionless. Therefore, using any consistent units for the factors which significantly affect this coefficient will not change the proposed equation to estimate sample size (Eq. 3.21).

- III. The margin of error of population maximum,  $MOE_{max}$ , is expressed as half of the confidence interval of the maximum and is given by:

$$MOE_{max} = \sigma^{-1} \left(1 - \frac{\alpha}{2}\right) \cdot SE_{max} \quad (3.15)$$

- IV. From Eq. 3.14 and Eq. 3.15, the coefficient of error of the maximum,  $COE_{max}$ , is given by:

$$\text{COE}_{\max} = \frac{\text{MOE}_{\max}}{\sigma^{-1} \left(1 - \frac{\alpha}{2}\right) \sigma_s} \quad (3.16)$$

V. The acceptable coefficient of error  $\text{COE}_{\text{accept}}$  is estimated from Eq. 3.16 corresponding to a pre-defined acceptable margin of error,  $\text{MOE}_{\text{accept}}$ , as follows:

$$\text{COE}_{\text{accept}} = \frac{\text{MOE}_{\text{accept}}}{\sigma^{-1} \left(1 - \frac{\alpha}{2}\right) \sigma_s} \quad (3.17)$$

VI. The bootstrap sample size,  $n_b$ , is plotted versus  $\text{COE}_{\max}$  estimated from Eq. 3.16. Then from this plot, the required sample size is obtained corresponding to the acceptable  $\text{COE}_{\text{accept}}$ .

### 3.3. Analysis of variance (ANOVA)

Analysis of variance was performed to check the significance of the factors that could affect the  $\text{COE}_{\max}$ . These factors are sample size ( $n$ ), population size ( $N$ ), sample mean ( $\mu_s$ ) and standard deviation ( $\sigma_s$ ). The levels of these factors used for ANOVA are shown in Table 3-1. The units of the mean and standard deviation are consistent.

**Table 3-1:** Factors levels.

Factor	Levels
Sample size, n	20, 40, 60, 80, 100
population size, N	$10^2, 10^3, 10^4, 10^5, 10^6, 10^7$
Sample mean, $\mu_s$	0.1, 100
Sample standard deviation, $\sigma_s$	0.1, 100

The ANOVA shows that the factors and factors interactions having a P-value less than a specified significance level  $\alpha$  (for example 0.01 or 0.05) are significant factors at confidence level  $(1-\alpha)$ . The analysis of variance results showed that sample size and population size have significant effect (P-value = 0.000) while mean and standard deviation have insignificant effect (P-value > 0.05) on COE<sub>max</sub>. When the effect of a factor depends on the level of another factor, it is said that the two factors interact. All factors interactions found with insignificant effect (P-value > 0.05) except the interaction of sample size and population size (P-value = 0.000). This conclusion about the significance of the effect of the factors and factors interactions on COE<sub>max</sub> was used to confirm the proposed equation to estimate sample size.

### **3.4. Proposed equation to estimate sample size**

Eq. 3.13 is used to estimate the required sample size for estimating the mean of a population of size  $N$  at a specified level of error. In the proposed methodology, our aim is to obtain an equation similar to Eq. 3.13 to estimate the required sample size to evaluate the population maximum instead of the population mean.

First we estimate the required sample size to evaluate the population mean using the proposed methodology in order to compare the results of the proposed methodology with the classical equation (Eq. 3.13). In this case step (viii) shown in Figure 3.1 was replaced with an estimate of the mean. Also, the maximum is replaced with the mean in steps (ix), (x), and (xi). An equation is fitted to the results obtained with the proposed methodology as follows:

- a) The sample mean and standard deviation are set at two levels (low and high) of 0.1 and 100 units. The scale and location parameters of Gumbel distribution are estimated for each sample.
- b) Bootstrap populations were generated following the sample Gumbel distribution with size,  $N$ , at levels of  $10^2, 10^3, 10^4, 10^5, 10^6$  and  $10^7$ .

- c) The COE<sub>mean</sub> is estimated for all possible combinations with different levels of sample mean ( $\mu_s$ ), standard deviation ( $\sigma_s$ ), population size (N), and bootstrap sample size  $n_b \leq N$ .
- d) The estimated COE<sub>mean</sub> is plotted versus bootstrap sample size  $n_b$  for different levels of population size N. For example, Figure 3-4 shows COE<sub>mean</sub> versus bootstrap sample size,  $n_b$ , for population size, N = 100 with two levels of  $\mu_s$  and  $\sigma_s$  are 0.1 and 100 units.
- e) The results of COE<sub>mean</sub> are fitted to the following equation:

$$\text{COE}_{\text{mean}} = \sqrt{\frac{1}{n} - \frac{1}{N}} \quad (3.18)$$

where COE<sub>mean</sub> is defined similar to Eq. 3.14 as follows:

$$\text{COE}_{\text{mean}} = \text{SE}_{\text{mean}} / \sigma_s \quad (3.19)$$

Also margin of error of the mean is expressed similar to Eq. 3.15 as follows:

$$\text{MOE}_{\text{mean}} = \Phi^{-1}\left(1 - \frac{\alpha}{2}\right) \cdot \text{SE}_{\text{mean}} \quad (3.20)$$

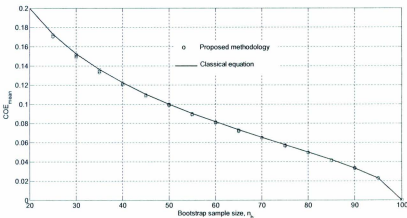


**Figure 3-4:**  $\text{COE}_{\text{mean}}$  versus bootstrap sample size,  $n_b$ , for population size,  $N = 100$ .

From Eqs. 3.18, 3.19 and 3.20, the proposed methodology yields the classical equation (Eq. 3.13). Thus, the sample size obtained using the proposed methodology is the same as the sample size obtained with the classical method when the sampling objective is to estimate the population mean.

The methodology is then extended to estimate the required sample size to evaluate the population maximum as shown in Figure 3.1. Then, an equation is fitted to the results. As it was done in case of the mean, the sample mean and standard deviation are set at two levels (low and high) of 0.1 and 100 units and the bootstrap populations were generated with size,  $N$ , at levels of  $10^2$ ,  $10^3$ ,  $10^4$ ,  $10^5$ ,

$10^6$  and  $10^7$ . The COE<sub>max</sub> is plotted versus bootstrap sample size n<sub>b</sub> for all possible combinations of sample mean ( $\mu_s$ ), sample standard deviation ( $\sigma_s$ ) and population size (N) at different levels. For example, Figure 3-5 shows COE<sub>max</sub> versus bootstrap sample size, n<sub>b</sub>, for population size, N =  $10^2$  and N =  $10^7$  respectively with two levels of  $\mu_s$  and  $\sigma_s$  are 0.1 and 100 units.

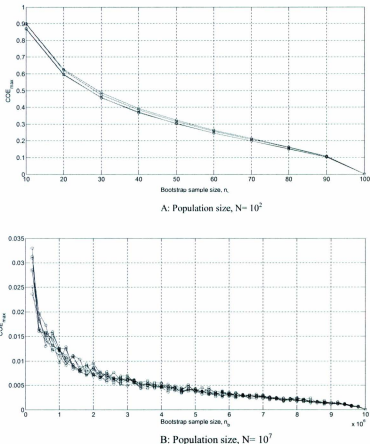


**Figure 3-5:** Bootstrap sample size,  $n_b$ , versus  $\text{COE}_{\max}$ .

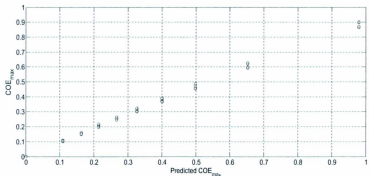
The results in Figure 3-5 show that the  $\text{COE}_{\max}$  is a function of the sample size and population size but not function of mean and standard deviation as it was evident by ANOVA. That means the  $\text{COE}_{\max}$  is not function of the inspection data. This fact is the significance of proposing the  $\text{COE}_{\max}$  in this work. Thus, Eq. 3.21

is general for any given localized corrosion data. The results of COE<sub>max</sub> are fitted to the following proposed equation (Eq. 3.21):

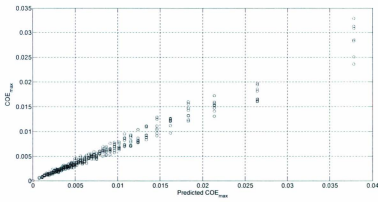
$$\text{COE}_{\text{max}} = f(N) \cdot \sqrt{\left(\frac{1}{n} - \frac{1}{N}\right)} \quad , N \leq 10^7 \quad (3.21)$$

$$\text{where } f(N) = \begin{cases} 1.3N^{0.2} & , N \leq 200 \\ 2.1N^{0.13} & , 200 < N \leq 10^4 \\ 3.2N^{0.083} & , 10^4 < N \leq 10^7 \end{cases}$$

It can be noted that Eq. 3.21 is similar to Eq. 3.18 except the function f(N). The predicted COE<sub>max</sub> using Eq. 3.21 is plotted in the horizontal axis versus the actual COE<sub>max</sub> obtained using the proposed methodology in the vertical axis for different possible combinations of the levels of bootstrap mean, standard deviation and population size. For example, Figure 3-6 shows this plot for population size, N = 10<sup>2</sup> and N = 10<sup>7</sup>.



A: Population size,  $N = 10^2$



B: Population size,  $N = 10^7$

**Figure 3-6:** Predicted versus actual  $\text{COE}_{\max}$ .

Figure 3-6 shows approximately a straight line with slope  $45^\circ$ . This means that the predicted and actual  $\text{COE}_{\max}$  are consistent.

From Eq. 3.21:

$$n = \frac{1}{\left(\frac{\text{COE}_{\max}}{f(N)}\right)^2 + \frac{1}{N}} \quad (3.22)$$

From Eq. 3.17 and Eq. 3.22, the sample size required to predict the population maximum with pre-defined  $\text{MOE}_{\text{accept}}$  can be calculated using the following equation:

$$n = \frac{1}{\left[\frac{\text{MOE}_{\text{accept}}}{f(N)\Phi^{-1}(1-\frac{\alpha}{2})\sigma_s}\right]^2 + \frac{1}{N}}, N \leq 10^7 \quad (3.23)$$

The estimated sample size using the proposed equation (Eq. 3.23) ensures that the predicted maximum localized corrosion using the extreme value method is within pre-defined  $\pm \text{MOE}_{\text{accept}}$  at a confidence level  $(1-\alpha)$ .

Table 3-2 shows a comparison of the proposed equation and classical equation to estimate sample size:

**Table 3-2:** Comparison of the proposed equation and classical equation.

	<b>Proposed equation (Eq. 3.23)</b>	<b>Classical equation (Eq. 3.13)</b>
	$n = \frac{1}{\left[ \frac{\text{MOE}_{\text{accept}}}{f(N) \cdot \Phi^{-1} \left( 1 - \frac{\alpha}{2} \right) \cdot \sigma_s} \right]^2 + \frac{1}{N}}, N \leq 10^7$	$n = \frac{\left[ \Phi^{-1} \left( 1 - \frac{\alpha}{2} \right) \cdot \left( \frac{\sigma}{\text{MOE}_{\text{accept}}} \right) \right]^2}{1 + \frac{\left[ \Phi^{-1} \left( 1 - \frac{\alpha}{2} \right) \cdot \left( \frac{\sigma}{\text{MOE}_{\text{accept}}} \right) \right]^2}{N}}$
<b>Sampling objective</b>	To estimate the population maximum	To estimate the population mean
<b>Method of estimation</b>	The population maximum is estimated with the extreme value method using a sample of size n	The population mean is estimated as the average of a sample of size n
<b>Precision</b>	The estimate error does not exceed a pre-defined MOE <sub>accept</sub> at a specified confidence level (1-α)	
<b>Sample size with same precision</b>	Larger	Smaller

### 3.5. Case study

Table 3-3 shows sample data of pitting corrosion in an offshore process piping. The data represent the maximum pit depth, x, measured using an ultrasonic inspection technique in 30 straight piping segments. These segments are selected randomly over the piping.

**Table 3-3:** Recorded maximum pit depth (in mm) in 30 inspected piping segments.

2	2	3.5	2	3.5	3.5	2	3.5	2	3
2.5	3	5	3.5	3.5	2	3	1	3.5	3
5	2.5	3	3.5	4.5	3	3.5	3.5	2	1

The proposed methodology was applied to estimate the sample size required to predict the maximum pit depth over the entire pipeline using the extreme value method within  $\pm 0.5\text{mm}$  (i.e.,  $\text{MOE}_{\text{accept}} = 0.5\text{mm}$ ) at 0.95 confidence level (i.e  $\alpha=0.05$ ) as follows:

Layering separation:

The total number of piping segments (population size,  $N$ ) is 100. These segments represent one group as they are similar and subjected to the same corrosion conditions.

Physical sampling:

The inspected segments are selected randomly over the piping.

Bootstrap sampling and extreme value analysis:

The data in Table 3-3 fits a straight line in the Gumbel probability plot as shown in Figure 3-7, thus this data fits Gumbel distribution. The Gumbel probability plot is obtained by plotting  $x$  versus  $[-\ln(-\ln(F(x)))]$ . The slope of the

straight line gives  $1/\theta$  and the intersection with the X-axis gives  $\lambda$ . The standard deviation of the sample data,  $\sigma_s$ , is estimated as 0.99 mm.

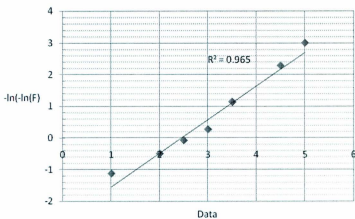
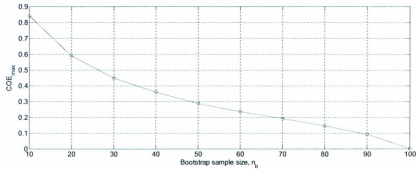


Figure 3-7: Gumbel probability plot of the inspection data.

Bootstrap samples with different sizes  $n_b \leq N$  are drawn from bootstrap populations randomly generated following the fitted Gumbel distribution. The maximum localized corrosion is predicted with extreme value method and the corresponding  $COE_{max}$  is estimated for each bootstrap sample.

The results of  $COE_{max}$  for different bootstrap sample sizes are shown in Figure 3-8.



**Figure 3-8:**  $\text{COE}_{\max}$  versus bootstrap sample size for population size of 100.

Sample size calculation:

From Eq. 3.18:

$$\text{COE}_{\text{accept}} = \text{MOE}_{\text{accept}} / \left[ \Phi^{-1} \left( 1 - \frac{\alpha}{2} \right) \cdot \sigma_z \right]$$

$$\text{COE}_{\text{accept}} = 0.5 / (1.96 * 0.99)$$

$$\text{COE}_{\text{accept}} = 0.26$$

From Figure 3-8, the bootstrap sample size at  $\text{COE}_{\text{accept}} = 0.26$  is 58.

The proposed equation (Eq. 3.24) can be used to calculate the sample size alternatively to the whole methodology as follows:

$$n = \frac{1}{\left[ \frac{\text{MOE}_{\text{accept}}}{f(N) \cdot \Phi^{-1}\left(1 - \frac{\alpha}{2}\right) \cdot \sigma_s} \right]^2 + \frac{1}{N}}$$

$$f(N) = 1.3N^{0.2} = 1.3 * 100^{0.2} = 3.265$$

$$n = \frac{1}{\left[ \frac{0.5}{3.265 * 1.96 * 0.99} \right]^2 + \frac{1}{100}} = 62$$

The obtained sample size using the methodology is close to the one obtained using the proposed equation.

The required sample size,  $n$ , to be inspected is assumed equal to the obtained bootstrap sample,  $n_b$ . The inspection is carried out for additional 28 segments (i.e., total  $n=58$  inspected segments). Table 3-4 shows the recorded maximum pit depth including all the 58 inspected pipeline segments.

**Table 3-4:** Maximum localized corrosion in 58 inspected piping segments in mm.

2	2	3.5	2	3.5	3.5	2	3.5	2	3
2.5	3	5	3.5	3.5	2	3	1	3.5	3
5	2.5	3	3.5	4.5	3	3.5	3.5	2	1
2.5	2	3.5	3.5	2.5	2	2.5	2	2	3
2	2.5	2.5	3	1.5	3.5	1	2.5	5	3
2	2.5	2	2.5	2	2	2.5	2		

The data shown in Table 3-4 fits Gumbel distribution with scale parameter 0.71mm and location parameter 2.31mm. The standard deviation of all inspection data shown in Table 3-4 is 0.91mm.

From Eq. 3.17, the COE<sub>accept</sub> is re-estimated based on the new data (Table 3-4) as 0.28 which corresponds to n<sub>b</sub>= 56 in Figure 3-8.

The required sample size n can also be obtained using the proposed equation (Eq. 3.21) which yields to:

$$n = \frac{1}{\left[ \frac{0.5}{3.265 * 1.96 * 0.91} \right]^2 + \frac{1}{100}} = 58$$

The number of inspected segments is 58 is not less than the estimated sample size, thus it is not required to inspect more piping segments.

Prediction of the maximum pit depth over the entire population (100 piping segments):

The maximum pit depth over the inspected sample is 5mm as shown in Table 3-4. The maximum pit depth over the entire population was predicted as 5.54mm by extrapolation of the Gumbel extreme value distribution of the inspection data in Table 3-4. The margin of error in this prediction is 0.5mm at 0.95 confidence level.

Sample size to estimate the mean:

If it is required to estimate the mean of the corrosion instead of the maximum based on the sample data shown in Table 3-3 with the same margin of error = 0.5mm and confidence level 0.95. Assuming that standard deviation of the sample (0.99 mm) is an approximation to standard deviation of the population ( $N=100$ ), the classical equation (Eq. 3.13) yields to sample size,  $n = 15$ . It can be noted that the sample size ( $n=15$ ) required to estimate the mean of population is much less than the sample size ( $n=58$ ) required to estimate the maximum of the same population with the same precision (i.e margin of error). Thus, the sampling strategy depends on what actually is investigated, for example, the mean or the maximum.

Effect of the population size:

In order to show the effect of the population size on the estimated sample size, it was assumed that the total number of segments of the pipeline (population size) is 1000 and the proposed methodology is reapplied for this population size.

Figure 3-9 shows  $\text{COE}_{\max}$  versus sample size for population size of 1000.

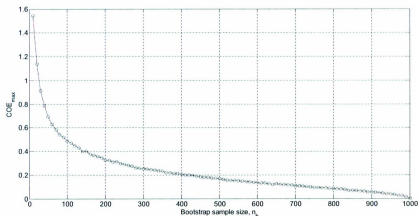


Figure 3-9:  $\text{COE}_{\max}$  versus sample size for population size of 1000.

From Figure 3-9, the sample size at  $\text{COE}_{\text{accept}} = 0.26$  is 278.

Using the proposed equation (Eq. 3.21):

$$f(N) = 2.1N^{0.13} = 2.1 * 1000^{0.13} = 5.155$$

$$n = \frac{1}{\left[ \frac{0.5}{5.155 * 1.96 * 0.99} \right]^2 + \frac{1}{1000}} = 286$$

The sample size is 58 when the population size is 100 (i.e., 58%) while it is 278 when the population size is 1000 (i.e., 27.8%) with the same acceptable margin of error (0.5mm) and at the same confidence level (0.95). Thus the larger the population size, the smaller the required sample size to population size ratio ( $n/N$ ). The larger population size can be obtained by reducing the unit inspection area ( $A_1$ ) to the limit that practically does not affect the detectability of the localized corrosion by the used inspection technique such as radiographic, ultrasonic or eddy current. The recommended practical inspection unit area can be obtained from the applicable codes such as API 570, API 579 and ASME, Section XI and ASTM G46-94.

### **3.6. Conclusion**

A methodology for calculating the sample size required to predict, with a specified precision, the maximum localized corrosion of process assets is proposed.

The proposed methodology is divided into main parts: i) layering separation, ii) physical sampling, ii) bootstrap sampling and extreme value analysis, and iv) calculation of sample size.

The results of the proposed methodology are used to fit an equation for calculation of sample size as a function of: the acceptable margin of error, the population size, the standard deviation of corrosion data and the required confidence level.

The estimated sample size ensures that the predicted maximum localized corrosion, determined using the extreme value method, is within an acceptable margin of error at a specified confidence level.

## **CHAPTER 4**

### **Inspection Sampling of Localized Corrosion- A Bayesian Approach<sup>3</sup>**

#### **Abstract**

The Bayesian updating approach and the extreme value method are integrated in a single algorithm to estimate the sample size required to assess, with a specified precision, localized corrosion of process assets.

Two closed-form formulas for calculating the sample size are obtained based on the proposed algorithm. One formula is to be used when prior information is available and the other when prior information is unavailable.

---

<sup>3</sup> Part of this chapter has been submitted for publication in a peer-reviewed journal "Khalifa, M., Khan, F. and Haddara, M. (2012). Inspection Sampling of Pitting Corrosion. Insight: Non-Destructive Testing and Condition Monitoring". To minimize repetition, the related references are listed in the thesis reference list.

#### **4.1 Introduction**

The objective of this chapter is to integrate the extreme value method and the Bayesian updating approach in a single algorithm to estimate the sample size required to assess localized corrosion of process assets.

The maximum localized corrosion over the entire asset and the corrosion rate are predicted at the inspection time using the extreme value method. The change over time in the maximum localized corrosion is evaluated based on the predicted corrosion rate.

The Bayesian updating approach is used to update prior information obtained from a previous inspection and engineering judgement once new inspection information is available. This allows the use of a smaller sample size than that obtained using the proposed methodology in Chapter 3 while guaranteeing the same precision.

A formula is introduced for estimating the standard error of the maximum localized corrosion predicted using the extreme value method. The margin of error is estimated as a multiple of the the standard error based on the required confidence level. The estimated sample size ensures that the posterior estimate of the maximum localized corrosion, predicted using the extreme value method, is within the acceptable margin of error.

## **4.2 The proposed algorithm**

The extreme value method is applied to predict the maximum localized corrosion size over the entire population,  $x_{\max}$  (Figure 3-3) assuming maximum corrosion size in each component/area fit a Gumbel extreme value distribution.

The predicted,  $x_{\max}$ , is expressed as a function of scale parameter, location parameter and population size.

Bayesian updating approach is used to obtain the posterior estimate of the mean and standard deviation of the maximum localized corrosion,  $x_{\max}$ , predicted with the extreme value method. The margin of error of the posterior mean of the predicted maximum corrosion over the entire population is estimated as a function of sample size, confidence level and posterior standard deviation of  $x_{\max}$ . The estimated margin of error should not be larger than the acceptable margin of error which leads to the required minimum sample size. The flowchart of the proposed algorithm is shown in Figure 4-1 and the details of the algorithm are explained hereafter.

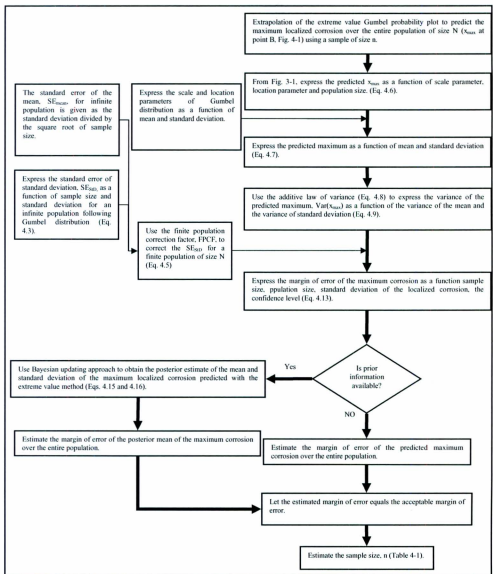


**Figure 4-1:** The flowchart of the proposed algorithm.

#### 4.2.1 Standard error of the standard deviation

The standard error of the sample mean,  $SE_{mean}$  for finite population is given by:

$$SE_{mean} = \frac{\sigma}{\sqrt{n}} \cdot FPCF \quad (4.1)$$

where  $\sigma$  is the standard deviation of the population and  $n$  is the sample size. FPCF is the finite population correction factor given by Eq. 2.6.

Eq. 4.1 is valid regardless of the type of the distribution provided that the sample size,  $n$ , is sufficiently large (Bernstein & Bernstein, 1999).

From Eqs. 4.1 and 2.6, the standard error of the mean is given by:

$$SE_{mean} = \sigma \cdot \sqrt{\frac{1}{n} - \frac{1}{N}} \quad (4.2)$$

There is no precise analytical formula available for estimating the standard error of a statistic other than the sample mean (Eq. 4.2). Figure 4-2 shows step-by-step procedure to obtain an approximate formula to estimate standard error of standard deviation for Gumbel and Normal distributions. This procedure can be extended to other distributions as well.

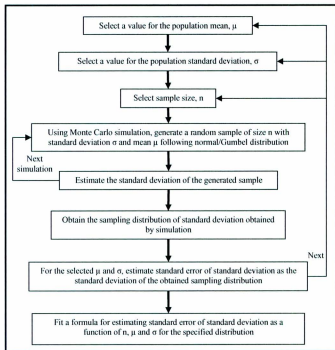


**Figure 4-2:** A procedure to obtain an approximate formula to estimate standard error of standard deviation.

Following the procedure shown in Figure 4-2, the standard error of standard deviation,  $SE_{StD}$ , is obtained for Normal and Gumbel distributions as follows:

For an infinite population following a Normal distribution:

$$SE_{StD, \text{Normal}} = 0.72 \frac{\sigma}{\sqrt{n}} \quad (4.3)$$

Using the  $FPCF = \sqrt{1 - n/N}$ , the  $SE_{StD}$  is obtained for a finite following a Normal distribution as follows:

$$SE_{StD, Normal} = 0.72 \frac{\sigma}{\sqrt{n}} \cdot FPCF = 0.72\sigma \cdot \sqrt{\frac{1}{n} - \frac{1}{N}} \quad (4.4)$$

Similarly, for a finite population following a Gumbel distribution:

$$SE_{StD, Gumbel} = \frac{\sigma}{\sqrt{n}} \cdot FPCF = \sigma \cdot \sqrt{\frac{1}{n} - \frac{1}{N}} \quad (4.5)$$

It may be noted from Eqs. 4.4 and 4.5 that the standard error is independent of the population mean,  $\mu$ .

The bootstrap simulation is used to validate Eqs. 4.4 and 4.5, as shown in Figure 4-3. The results of  $SE_{StD, Gumbel}$  obtained using bootstrap simulation are consistent with those obtained using the approximate formula (Eq. 4.5). For example, Figure 4-4 shows a comparison of the  $SE_{StD, Gumbel}$  for population size  $N=10^3$  and  $N=10^{11}$ , sample size  $n = 20$  to 200 and population standard deviation,  $\sigma = 1$  to 100 unit.

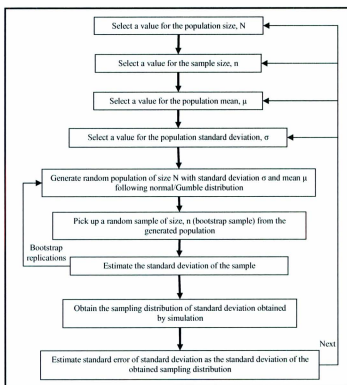


**Figure 4-3:** Using bootstrap sampling to validate the obtained approximate formula to estimate standard error of standard deviation.

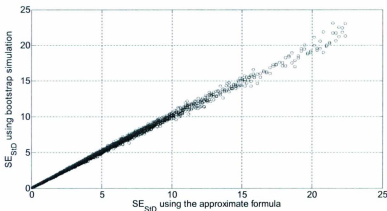


**Figure 4-4:**  $SE_{SID, \text{Gumbel}}$  obtained with the proposed formula (Eq. 4.5) versus  $SE_{SID, \text{Gumbel}}$  obtained with bootstrap simulation.

#### 4.2.2 Standard error of the maximum corrosion predicted using the extreme value method

The predicted maximum corrosion,  $x_{\max}$ , over the entire population corresponding to point B (Figure 3-3) can be estimated as follows:

$$x_{\max} = \lambda + \theta \ln \left( -\ln \frac{N}{N+1} \right) \quad (4.6)$$

Using Eqs. 3.5 and 3.6; and substituting  $\lambda$  and  $\theta$  in terms of the sample estimate of  $\mu$  and  $\sigma$  in Eq. 4.6, one gets:

$$x_{\max} = \mu - \frac{\sqrt{6}}{\pi} \left( \gamma + \ln \left( -\ln \frac{N}{N+1} \right) \right) \cdot \sigma \quad (4.7)$$

The additive law of the variance of random variables X and Y is expressed as follows:

$$Var(aX + bY) = a^2.Var(X) + b^2.Var(Y) + 2a.b.Cov(X,Y) \quad (4.8)$$

where a and b are constants and Cov(X,Y) is the covariance of X and Y.

As  $\mu$  and  $\sigma$  of normally distributed data are uncorrelated random variables, that is, their covariance is zero; the variance of  $x_{max}$  is estimated using Eqs. 4.7 and 4.8 as follows:

$$Var(x_{max}) = \sigma_{x_{max}}^2 = Var(\mu) + \left[ \frac{\sqrt{6}}{\pi} \left( \gamma + \ln \left( -\ln \frac{N}{N+1} \right) \right) \right]^2 . Var(\sigma) \quad (4.9)$$

Substituting Eqs. 4.2 and 4.5 in Eq. 4.9 where  $Var(\mu) = (SE_{mean})^2$  and  $Var(\sigma) = (SE_{Std})^2$ , the variance of the predicted maximum corrosion size,  $x_{max}$ , (for Gumble distribution) is given by:

$$Var(x_{max}) = \sigma_{x_{max}}^2 = \left[ 1 + \frac{6}{\pi^2} \left( \gamma + \ln \left( -\ln \frac{N}{N+1} \right) \right)^2 \right] . \sigma^2 . \left( \frac{1}{n} - \frac{1}{N} \right) \quad (4.10)$$

From Eq. 4.10, the standard error of the predicted  $x_{max}$ , is given by:

$$SE_{max} = \sigma_{x_{max}} = MVCF . \sigma . \sqrt{\frac{1}{n} - \frac{1}{N}} \quad (4.11)$$

where MVCF is referred in this work as the maximum value correction factor for Gumbel distribution and given by:

$$MVCF = \sqrt{1 + \frac{6}{\pi^2} \left( \gamma + \ln \left( -\ln \frac{N}{N+1} \right) \right)^2} \quad (4.12)$$

It may be noted that the standard deviation in Eq. 4.11 is corrected by the MVCF when estimating the standard error of the maximum value instead of the mean (Eq. 4.2) for a finite population following a Gumbel distribution.

#### 4.2.3 Calculation of sample size

##### 4.2.3.1. Without having prior information

The margin of error of the predicted maximum corrosion size,  $MOE_{max}$ , is given by Eq. 3.15.

Let  $MOE_{max}$  in Eq. 3.15 equals the acceptable margin of error,  $MOE_{accept}$ , and substitute for  $SE_{max}$  from Eq. 4.10 as follows:

$$MOE_{accept} = \Phi^{-1} \left( 1 - \frac{\alpha}{2} \right) \cdot MVCF \cdot \sigma \cdot \sqrt{\left( \frac{1}{n} - \frac{1}{N} \right)} \quad (4.13)$$

This leads to a sample size  $n$  given by the following formula:

$$n = \frac{\left[ \Phi^{-1}\left(1 - \frac{\alpha}{2}\right) \left( \frac{\sigma_{MVCF}}{MOE_{accept}} \right) \right]^2}{1 + \frac{\left[ \Phi^{-1}\left(1 - \frac{\alpha}{2}\right) \left( \frac{\sigma_{MVCF}}{MOE_{accept}} \right) \right]^2}{N}} \quad (4.14)$$

#### 4.2.3.2. Having prior information

Eq. 4.14 estimates the sample size based on the available information obtained in the current inspection without using any prior information that may be available from previous inspections and/or engineering judgment. It is useful to use prior information obtained from previous inspections along with new information obtained from the current inspection. This allows using a sample of smaller size in the current inspection to provide an estimate of the maximum localized corrosion with the same precision (i.e., margin of error) at the same confidence level. The prior information is updated once newly obtained information is available using Bayesian theory.

It should be noted that the maximum corrosion size in each inspected component/area,  $x$ , is assumed to follow a Gumbel distribution while the maximum corrosion size over the entire population,  $x_{max}$ , (predicted with the extreme value method) is assumed to follow a normal distribution. The rational of this assumption is that considering the extreme value method as a tool to measure  $x_{max}$ ; in this case, it is reasonable to assume that the measured  $x_{max}$  is normally distributed. The posterior estimate for the mean and the standard deviation of a

normally distributed random variable are obtained from Bayes' theorem as follows (Bernstein & Bernstein, 1999):

$$x_{\max}^* = \frac{x_{\max} (\sigma_{x_{\max}}')^2 + x'_{\max} (\sigma_{x_{\max}})^2}{(\sigma_{x_{\max}}')^2 + (\sigma_{x_{\max}})^2} \quad (4.15)$$

$$\sigma_{x_{\max}}'' = \sqrt{\frac{(\sigma_{x_{\max}}')^2 \cdot (\sigma_{x_{\max}})^2}{(\sigma_{x_{\max}}')^2 + (\sigma_{x_{\max}})^2}} \quad (4.16)$$

where  $x_{\max}$  is the maximum corrosion size over the entire population predicted with the extreme value method and  $\sigma_{x_{\max}}$  is the standard deviation of  $x_{\max}$ .  $x'_{\max}$  and  $\sigma_{x_{\max}}'$  are the prior mean and standard deviation of  $x_{\max}$ , respectively.  $x_{\max}$  is estimated with the extreme value method as shown in Figure 3-3 using the current inspection sample.  $\sigma_{x_{\max}}$  is estimated as given by Eq. 4.10.  $x'_{\max}$  is estimated based on the last updated  $x_{\max}$  (the posterior estimate of the maximum corrosion size in the previous inspection,  $x_{\max}^{o''}$ ) considering the corrosion rate, CR, as follows:

$$x'_{\max} = x_{\max}^{o''} + CR \cdot t_{int} \quad (4.17)$$

where  $t_{int}$  is the interval between the current inspection and the previous inspection.

$\sigma'_{x_{max}}$  is obtained using Eq. 4.17 and the additive law of variance (Eq. 4.8) assuming  $x_{max}^o$  and CR are uncorrelated random variables as follows:

$$\sigma'_{x_{max}} = \sqrt{\sigma_{x_{max}^o}^{-2} + t_{int}^2 \cdot \sigma_{CR}^2} \quad (4.18)$$

From Eq. 4.16, the posterior standard deviation of maximum localized corrosion over the entire population in the previous inspection,  $\tilde{\sigma}_{x_{max}^o}$ , is given by:

$$\tilde{\sigma}_{x_{max}^o} = \sigma_{x_{max}^o} \cdot \sqrt{\frac{(\sigma'_{x_{max}})^2}{(\sigma'_{x_{max}})^2 + (\sigma_{x_{max}^o})^2}} \quad (4.19)$$

From Eq. 4.19,  $\tilde{\sigma}_{x_{max}^o}$  is equal to  $\sigma_{x_{max}^o}$  multiplied by a factor less than 1; thus  $\tilde{\sigma}_{x_{max}^o} < \sigma_{x_{max}^o}$ . Since sample size increases as the standard deviation increases, conservatively substitute  $\tilde{\sigma}_{x_{max}^o} = \sigma_{x_{max}^o}$  in Eq. 4.18 yields:

$$\sigma'_{x_{max}} = \sqrt{\sigma_{x_{max}^o}^2 + t_{int}^2 \cdot \sigma_{CR}^2} \quad (4.20)$$

From Eq. 4.12:

$$\sigma_{x_{max}^o} = MVCF \cdot \sigma_o \cdot \sqrt{\frac{1}{n_o} - \frac{1}{N}} \quad (4.20)$$

where  $\sigma_0$  and  $n_0$  are standard deviation of the maximum corrosion recorded for each component/area and sample size (number of recorded maxima) in the previous inspection, respectively.

Kowaka et al. (1984) suggested that the corrosion rate is to be estimated based on the maximum localized corrosion over the entire population predicted with the extreme value method in the last two consecutive inspections and the inspection interval. Therefore, the corrosion rate is given by, see Figure 4-5:

$$CR = \frac{x_{max} - x_{max}^0}{t_{int}} \quad (4.21)$$

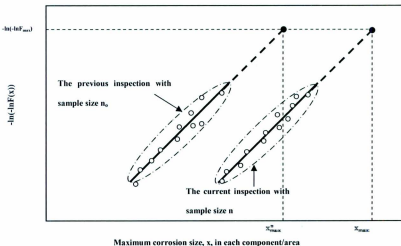


**Figure 4-5:** The corrosion rate estimation with the extreme value method as suggested by Kowaka et al. (1984).

Substituting CR from Eq. 4.22 in Eq. 4.17:

$$\dot{x}_{max} = \overset{\circ}{x_{max}} + x_{max} - \overset{\circ}{x_{max}} \quad (4.23)$$

The variance of the corrosion rate,  $\sigma_{CR}^2$ , can be obtained from Eq. 4.22 and the additive law of variance, assuming  $x_{max}$  and  $\overset{\circ}{x_{max}}$  are uncorrelated random variables, as follows:

$$\sigma_{CR}^2 = \frac{1}{t_{int}^2} [\sigma_{x_{max}}^2 + \sigma_{\overset{\circ}{x_{max}}}^2] \quad (4.24)$$

Substituting  $\sigma_{x_{max}}$  and  $\sigma_{\overset{\circ}{x_{max}}}$  from Eqs. 4.10 and 4.21 in Eq. 4.24:

$$\sigma_{CR}^2 = \frac{MVCF^2}{t_{int}^2} \left[ \sigma^2 \cdot \left( \frac{1}{n} - \frac{1}{N} \right) + \sigma_o^2 \cdot \left( \frac{1}{n_o} - \frac{1}{N} \right) \right] \quad (4.25)$$

Substituting  $\sigma_{CR}$  from Eq. 4.25 and  $\overset{\circ}{x_{max}} = \sigma_{\overset{\circ}{x_{max}}}$  from Eq. 4.21 in Eq. 4.18:

$$\dot{x}_{max} = MVC \sqrt{\left[ \sigma^2 \cdot \left( \frac{1}{n} - \frac{1}{N} \right) + 2\sigma_o^2 \cdot \left( \frac{1}{n_o} - \frac{1}{N} \right) \right]} \quad (4.26)$$

Substituting  $\dot{x}_{max}$ ,  $\sigma_{x_{max}}$  and  $x_{max}$  from Eqs. 4.26, 4.11 and 4.17 in Eqs. 4.15 and 4.16:

$$\dot{x}_{max} = MVC \cdot \sqrt{\frac{\sigma^2 \cdot \left( \frac{1}{n} - \frac{1}{N} \right) \left[ \sigma^2 \cdot \left( \frac{1}{n} - \frac{1}{N} \right) + 2\sigma_o^2 \cdot \left( \frac{1}{n_o} - \frac{1}{N} \right) \right]}{\sigma^2 \cdot \left( \frac{1}{n} - \frac{1}{N} \right) + \left[ \sigma^2 \cdot \left( \frac{1}{n} - \frac{1}{N} \right) + 2\sigma_o^2 \cdot \left( \frac{1}{n_o} - \frac{1}{N} \right) \right]}} \quad (4.27)$$

$$\bar{x}_{max} = \frac{x_{max}[\sigma^2(\frac{1}{n} - \frac{1}{N}) + 2\sigma_o^2(\frac{1}{n_o} - \frac{1}{N})] + (x_{max}^{o'} + x_{max} - x_{max}^o)\sigma^2(\frac{1}{n} - \frac{1}{N})}{2\sigma^2(\frac{1}{n} - \frac{1}{N}) + 2\sigma_o^2(\frac{1}{n_o} - \frac{1}{N})} \quad (4.28)$$

The sample size should satisfy the condition that the margin of error of the posterior estimate of the mean of the maximum corrosion,  $\bar{x}_{max}$ , does not exceed the acceptable margin of error  $MOE_{accept}$  as follows:

$$MOE = \Phi^{-1}\left(1 - \frac{\alpha}{2}\right) \cdot \sigma_{\bar{x}_{max}} = MOE_{accept} \quad (4.29)$$

From Eqs. 4.2 and 4.29, sample size for the extreme value analysis of localized corrosion (in case prior information is available) is given by the following formula:

$$MOE_{accept} = \Phi^{-1}(1 - \alpha/2) \cdot MVCF \cdot \sqrt{\frac{\sigma^2(\frac{1}{n} - \frac{1}{N})[\sigma^2(\frac{1}{n} - \frac{1}{N}) + 2\sigma_o^2(\frac{1}{n_o} - \frac{1}{N})]}{\sigma^2(\frac{1}{n} - \frac{1}{N}) + [\sigma^2(\frac{1}{n} - \frac{1}{N}) + 2\sigma_o^2(\frac{1}{n_o} - \frac{1}{N})]}} \quad (4.30)$$

Table 4-1 summarizes the proposed formulas to calculate sample size for the extreme value analysis of localized corrosion.

**Table 4-1:** Sample size calculation for the extreme value analysis of localized corrosion.

Case	Formula for sample size calculation	Posterior mean and standard deviation of the maximum localized corrosion $x_{max}$
1-Without having prior information	$n = \frac{\left[ \phi^{-1}\left(1 - \frac{\alpha}{2}\right) \left( \frac{\sigma_{MVCF}}{MOE_{accept}} \right) \right]^2}{1 + \left[ \frac{\phi^{-1}\left(1 - \frac{\alpha}{2}\right) \left( \frac{\sigma_{MVCF}}{MOE_{accept}} \right)}{N} \right]^2}$	$\bar{x}_{max} = x_{max}$ $\sigma_{x_{max}} = \sigma_{x_{max}} = MVCF \cdot \sigma_{\sigma} \sqrt{\left(\frac{1}{n} - \frac{3}{N}\right)}$
2- Having prior information	$MOE_{accept} = \phi^{-1}\left(1 - \frac{\alpha}{2}\right) \cdot MVCF \cdot \sqrt{\frac{\sigma^2\left(\frac{1-\beta}{n}-\frac{1}{N}\right)\left[\sigma^2\left(\frac{1-\beta}{n}-\frac{1}{N}\right)-2\sigma^2\left(\frac{1-\beta}{n}\right)\right]}{\sigma^2\left(\frac{1-\beta}{n}\right)+\sigma^2\left(\frac{1-\beta}{n}-\frac{1}{N}\right)-2\sigma^2\left(\frac{1-\beta}{n}\right)}}$ <p>where</p> $MVCF = \sqrt{1 + \frac{6}{z^2} \left( \gamma + \ln \left( -\ln \frac{N}{N+1} \right) \right)^2}$	$\bar{x}_{max} = \frac{x_{max} \left[ \sigma^2\left(\frac{1-\beta}{n}\right) + 2\sigma^2\left(\frac{1-\beta}{n}-\frac{1}{N}\right) \right] + \left( x_{max}^2 + x_{max} - x_{max}^2 \right) \cdot \sigma^2\left(\frac{1-\beta}{n}\right)}{2\sigma^2\left(\frac{1-\beta}{n}\right) + 2\sigma^2\left(\frac{1-\beta}{n}-\frac{1}{N}\right)}$ $\sigma_{x_{max}} = MVCF \cdot \sqrt{\frac{\sigma^2\left(\frac{1-\beta}{n}\right)\left[\sigma^2\left(\frac{1-\beta}{n}\right)+2\sigma^2\left(\frac{1-\beta}{n}\right)\right]}{\sigma^2\left(\frac{1-\beta}{n}\right)\left[\sigma^2\left(\frac{1-\beta}{n}\right)+2\sigma^2\left(\frac{1-\beta}{n}\right)\right]}}$

It may be noted that when no prior information is available, this is equivalent to  $\sigma_0$  approaches infinity; Eq. 4.30 yields to Eq. 4.13. Therefore, the formula for the sample size in case 2 yields to the formula of sample size in case 1. Also, the estimated sample size using Eq. 4.14 (Case 1) is consistent with the estimated sample size using Eq. 3.23.

#### 4.3 Prediction of the maximum localized corrosion in future time

The maximum corrosion size is extrapolated over the total area of population to predict the maximum corrosion size over the entire population,  $x_{max}$  as shown in

Figure 4-1. It is also useful to extrapolate  $x_{max}$  in time to predict any future change in the condition of the asset. The linear extrapolation of  $x_{max}$  in time is used in this work.

As the corrosion flaw size grows with time, the parameters of the normal distribution (mean and standard deviation) of the predicted  $x_{max}$ , change. The change in the mean and standard deviation of  $x_{max}$  after a period of time  $\Delta t$  from the current inspection is estimated as follows:

$$x_{max,\Delta t} = x_{max} + CR \cdot \Delta t \quad (4.31)$$

$$\sigma_{x_{max,\Delta t}} = \sqrt{\sigma_{x_{max}}^2 + \sigma_{CR}^2 \cdot (\Delta t)^2} \quad (4.32)$$

Substituting  $\sigma_{CR}$  from Eq. 4.25:

$$\sigma_{x_{max,\Delta t}} = \sqrt{\sigma_{x_{max}}^2 + MVCF^2 \cdot \left(\frac{\Delta t}{t_{int}}\right)^2 \cdot \left[\sigma^2 \cdot \left(\frac{1}{n} - \frac{1}{N}\right) + \sigma_\sigma^2 \cdot \left(\frac{1}{n_\sigma} - \frac{1}{N}\right)\right]} \quad (4.33)$$

Substituting  $\sigma_{x_{max}}^2$  from Eq. 4.11:

$$\sigma_{x_{max,\Delta t}} = MVCF \sqrt{\sigma^2 \cdot \left(\frac{1}{n} - \frac{1}{N}\right) + \left(\frac{\Delta t}{t_{int}}\right)^2 \cdot \left[\sigma^2 \cdot \left(\frac{1}{n} - \frac{1}{N}\right) + \sigma_\sigma^2 \cdot \left(\frac{1}{n_\sigma} - \frac{1}{N}\right)\right]} \quad (4.34)$$

Eqs. 4.31 and 4.34 can be used to predict the maximum corrosion after a period of time  $\Delta t$  from the current inspection. From Eqs. 4.32 and 4.33, the mean and standard deviation of the predicted maximum corrosion size over the population are increasing with increasing  $\Delta t$ . The distribution of the predicted maximum corrosion,  $x_{max}$ , after a period of time  $\Delta t$  is Normal with mean  $x_{max,\Delta t}$  and standard deviation  $\sigma_{x_{max,\Delta t}}$ .

#### 4.4 Case study

A pipeline subjected to localized corrosion is considered in this case study. The pipeline is divided into 100 similar segments (population size,  $N = 100$ ). Assume the standard deviation of the maximum corrosion size in each pipeline segment,  $x$ , is  $\sigma = 2$  mm and  $\sigma_0 = 1$  mm in the current and the previous inspection, respectively. Assume further that the random variable  $x$  follows Gumbel extreme value distribution. The acceptable margin of error,  $MOE_{accept}$ , is taken in this example as 0.5 mm at a confidence level  $(1-\alpha) = 0.95$ .

It is required to estimate the sample size to assess the localized corrosion of this pipeline in the current inspection and previous inspection. Also, it is required to estimate the posterior mean of the maximum corrosion size over the entire pipeline assuming:

- The maximum corrosion size predicted with the extreme value method in the previous inspection is  $x_{\max}^0 = 4.5$  mm and in the current inspection is  $x_{\max} = 5$  mm.
- The posterior mean of the maximum corrosion size estimated in the previous inspection,  $x_{\max}^{0*}$ , is 4.8 mm.
- The inspection interval,  $t_{int}$ , between the current inspection and previous inspection is one year.

For the previous inspection (no prior information):

Using the proposed formula (Case 1, Table 4-1):

$$n = \frac{\left[ \Phi^{-1} \left( 1 - \frac{\alpha}{2} \right) \cdot \left( \frac{\sigma_{MVCF}}{MOE_{accept}} \right) \right]^2}{1 + \frac{\left[ \Phi^{-1} \left( 1 - \frac{\alpha}{2} \right) \cdot \left( \frac{\sigma_{MVCF}}{MOE_{accept}} \right) \right]^2}{N}}$$

$$MVCF = \sqrt{1 + \frac{6}{\pi^2} \left( \gamma + \ln \left( -\ln \frac{N}{N+1} \right) \right)^2} = \sqrt{1 + \frac{6}{\pi^2} \left( 0.577 + \ln \left( -\ln \frac{100}{100+1} \right) \right)^2} = 3.30$$

$$n = \frac{[1.96 * 1 * 3.30 / 0.5]^2}{1 + \frac{[1.96 * 1 * 3.30 / 0.5]^2}{100}} = 63$$

Assuming the pipeline was divided into more segments, Table 4-2 shows sample size for different values of population size N (total number of segments).

**Table 4-2:** Sample size in the previous inspection for different values of population size N.

Population size, N	Sample size, n (Case 1, Table 4-1)	% (n/N)
$10^2$	63	63%
$10^3$	281	28%
$10^4$	665	7%

From Table 4-2, the sample size increases as the population size increases. The percentage of sample size to population size decreases as the population size increases. Therefore, it recommended dividing the pipeline into the maximum possible number of segments. The minimum area of the segment is dependent on the inspection tool and the required area to cover the maximum corrosion size in each segment.

For the current inspection:

The prior information of sample size,  $n_0$ , and standard deviation of the maximum corrosion in each segment ( $\sigma_0 = 1 \text{ mm}$ ) are known from the previous inspection. To determine the sample size, the proposed formulas (Table 4-1) are applied as follows:

Case 1 (no prior information is available):

$$n = \frac{[1.96 * 1 * MVCF / 0.5]^2}{1 + \frac{[1.96 * 1 * MVCF / 0.5]^2}{N}}$$

Case 2 (prior information is available from previous inspection):

$$0.5 = 1.96 * MVCF * \sqrt{\frac{2^2 \left(\frac{1}{n} - \frac{1}{N}\right) [2^2 \left(\frac{1}{n} - \frac{1}{N}\right) + 2 * 1^2 * \left(\frac{1}{n_0} - \frac{1}{N}\right)]}{2^2 \left(\frac{1}{n} - \frac{1}{N}\right) + [2^2 \left(\frac{1}{n} - \frac{1}{N}\right) + 2 * 1^2 * \left(\frac{1}{n_0} - \frac{1}{N}\right)]}}$$

The required sample size,  $n$ , is estimated using the above two equations for different values of population size and given in Table 4-3.

**Table 4-3:** Sample size and the posterior estimate of the mean of the maximum corrosion size.

Population size, N	Sample size, $n_0$ (previous inspection, Table 4-2)	Sample size, n (current inspection)			Posterior estimate of the mean of the maximum corrosion, $x_{\max}$ (current inspection) in mm	
		Without prior information (Case 1, Table 4-1)	With prior information (Case 2, Table 4-1)	% Saving	Without prior information (Case 1, Table 4-1)	With prior information (Case 2, Table 4-1)
$10^3$	63	88	83	6%	5	5.09
$10^3$	281	610	525	14%	5	5.09
$10^4$	665	2218	1677	24%	5	5.09

From Table 4-3, the sample size with prior information is less than the sample size with no prior information with the same margin of error at the same

confidence level. This shows the advantage of updating the prior information once new information is available. The percentage saving in sample size in case 1 (with prior information) in comparison to case 2 (without prior information) increases as population size increases.

The posterior estimate of the maximum corrosion size:

The posterior mean of the maximum corrosion size,  $\bar{x}_{\max}$ , is estimated as follows:

For the previous inspection:

$\bar{x}_{\max}$  equals the predicted maximum corrosion size,  $x_{\max} = 5$  mm (Table 4-1, Case 1).

For the current inspection:

The posterior mean of the maximum corrosion size,  $\bar{x}_{\max}$  is estimated using the formula shown in Table 4-1 (Case 2) as follows:

$$x''_{\max} = \frac{x_{\max} \cdot \left[ \sigma^2 \cdot \left( \frac{1}{n} - \frac{1}{N} \right) + 2\sigma_o^2 \cdot \left( \frac{1}{n_o} - \frac{1}{N} \right) \right] + (x''_{\max} + x_{\max} - x''_{\max}) \cdot \sigma^2 \cdot \left( \frac{1}{n} - \frac{1}{N} \right)}{2\sigma^2 \cdot \left( \frac{1}{n} - \frac{1}{N} \right) + 2\sigma_o^2 \cdot \left( \frac{1}{n_o} - \frac{1}{N} \right)}$$

$$x''_{\max} = \frac{5 * \left[ 2^2 * \left( \frac{1}{n} - \frac{1}{N} \right) + 2 * 1^2 * \left( \frac{1}{n_0} - \frac{1}{N} \right) \right] + (4.8 + 5 - 4.5) * 2^2 * \left( \frac{1}{n} - \frac{1}{N} \right)}{2 * 2^2 * \left( \frac{1}{n} - \frac{1}{N} \right) + 2 * 1^2 * \left( \frac{1}{n_0} - \frac{1}{N} \right)}$$

The results of  $x''_{\max}$  are obtained using the above equation for different values of N and the corresponding  $n_0$  and n as shown in Table 4-4.

The margin of error, MOE, and the upper limit of the posterior estimate of the maximum corrosion,  $x''_{\max}$ , at a specified confidence level of 95% for different sample sizes (assuming population size, N = 1000) are shown in Figure 4-7. The margin of error, MOE, is estimated using Eq. 4.29 and the upper limit is estimated as ( $x''_{\max}$ +MOE).

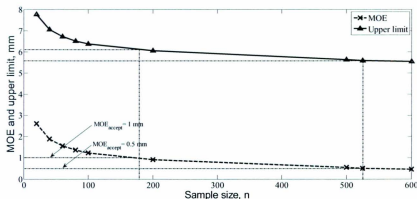


**Figure 4-6:** The margin of error, MOE, and the upper limit of the posterior estimate of the maximum corrosion at a confidence level of 95%.

From Figure 4-7, the upper limit and MOE of the posterior estimate of the maximum corrosion decrease as sample size increases. Sample size is affected by the acceptable margin of error,  $MOE_{accept}$ . For example, if  $MOE_{accept} = 0.5$  mm, a sample size of 525 is appropriate while if  $MOE_{accept} = 1$  mm, a sample size of 180 is appropriate as shown in Figure 4-7. Engineering judgment should be made to decide the acceptable margin of error in the light of the tolerance between the upper limit and the critical corrosion size to failure.

The corrosion rate, CR, is estimated using Eq. 4.22 as follows:

$$CR = \frac{x_{max} - x_{max}^0}{t_{int}} = \frac{5 - 4.5}{1} = 0.5 \text{ mm/year}$$

The mean and standard deviation of the maximum corrosion size over the population after a period of time  $\Delta t$  from the current inspection are estimated using Eqs. 4.31 and 4.34 and shown in Table 4-4.

**Table 4-4:** Mean and standard deviation of the maximum corrosion size over the population ( $x_{\max,\Delta t}$  and  $\sigma_{x_{\max,\Delta t}}$ ) for different periods of time after the current inspection ( $\Delta t$ ).

$\Delta t$ (Year)	$x_{\max,\Delta t}$ (mm)	$\sigma_{x_{\max,\Delta t}}$ (mm)					
		N=10 <sup>2</sup>		N=10 <sup>3</sup>		N=10 <sup>4</sup>	
		n=83	n=42	n=525	n=263	n=1677	n=839
0	5	0.30	0.78	0.30	0.53	0.30	0.45
1	5.5	0.56	1.16	0.56	0.84	0.56	0.73
2	6	0.98	1.88	0.99	1.39	0.99	1.24
3	6.5	1.44	2.68	1.45	2.00	1.45	1.79
4	7	1.90	3.51	1.91	2.63	1.91	2.35
5	7.5	2.36	4.35	2.38	3.26	2.38	2.92

#### 4.5 Conclusion

An algorithm that integrates the extreme value method and Bayesian updating method has been proposed to estimate the sample size required to assess, with a specified precision, localized corrosion of process assets.

The extreme value method is used to predict maximum corrosion over the entire asset. The Bayesian updating method is used to update prior information obtained from previous inspections and engineering judgement once newly obtained information is available. This allows the use of a smaller sample size with the same precision. The precision is quantified in terms of a margin of error

of the extreme value prediction of the maximum corrosion size over the entire asset.

Two closed-form formulas for calculating the sample size are obtained. The two formulas address the two situations when prior information is available or is not available.

The application of this algorithm is explained through a case study of localized corrosion in a pipeline, in which the estimated sample size is up to 24% less when using available prior information than when prior information is unavailable.

## **CHAPTER 5**

### **Optimization of the Risk-Based Inspection and Maintenance (RBIM)**

#### **Plan<sup>4</sup>**

##### **Abstract**

A quantitative risk-based inspection and maintenance methodology (RBIM) is proposed for optimal inspection and maintenance planning. To solve the optimization problem, an objective function is formulated as a function of the present value of inspection cost, repair/replacement cost, risk of failure and the remaining value of the asset after a specified period of time. The selection of the optimum inspection interval and maintenance activity is based on minimizing the objective function subject to a constraint that the risk of failure over the asset's lifetime does not exceed an acceptable level. The proposed methodology allows minimizing the cost of inspection and maintenance over the lifetime of a deteriorated asset/system without compromising the safety.

---

<sup>4</sup> Part of this chapter has been submitted and under review in a peer-reviewed journal "Khalifa, M., Khan, F. and Haddara, M. (2011). Optimal risk-based inspection and maintenance planning for process assets. The journal of quality in maintenance Engineering". To minimize repetition, the related references are listed in the thesis reference list.

## **5.1 Introduction**

Inspection is carried out at pre-defined intervals and prescribed locations. This monitoring strategy is needed to ensure that all assets perform their intended functions and that plant integrity is not threatened. Based on the outcomes of the inspection, a maintenance decision such as repair or replacement is made. An inspection and maintenance plan involves the selection of inspection intervals and a required maintenance strategy, such as repair or replacement. Inspection and maintenance are planned using one or more of the approaches: remaining life-based approach, reliability-based approach and risk-based approach.

The objective of this chapter is to develop a quantitative RBIM methodology for optimal inspection and maintenance planning for process assets subjected to fatigue and corrosion. The proposed methodology would contribute to well informed inspection and maintenance decisions to enhance safety and integrity of process assets, with optimal utilization of physical and financial resources.

## **5.2 The Proposed RBIM Methodology**

Figure 5-1 shows the proposed methodology flowchart.

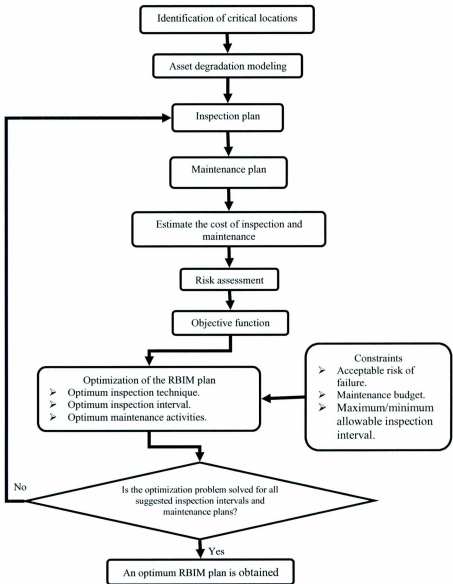


**Figure 5-1:** The proposed methodology flowchart.

The main steps of the proposed methodology are as follows:

**5.2.1** Classification of asset's components/areas according to criticality of deterioration

Each group of components/areas obtained through layering separation (Section 3.2.1) is classified into categories according to the consequences of failure. An inspection and maintenance plan is considered for each category.

**5.2.2** Asset degradation modeling

The aim of this step is to evaluate the flaw size and its growth rate due to fatigue and corrosion at any time, t.

Fatigue crack growth is modeled using the well known Paris Law (1963) which relates crack growth to the number of stress cycles as follows:

$$\frac{da}{dN_c} = C(\Delta k)^m \quad (5.1)$$

where a is the crack size, N<sub>C</sub> is the number of stress cycles, C and m are material parameters for fatigue crack growth rate in a specified environment and Δk is the stress intensity range factor which, in general, can be calculated as follows:

$$\Delta k = Y(a) \Delta \sigma \sqrt{\pi a} \quad (5.2)$$

where  $\Delta\sigma$  is the applied stress range and  $Y(a)$  is the geometry function.

An integral form of Paris Law is given by:

$$N_C = \int_{a_0}^{a_N} \frac{da}{C[\Delta\sigma Y(a) \sqrt{\pi a}]^m} \quad (5.3)$$

where  $a_0$  is the initial crack size;  $a_N$  is crack size after  $N_C$  stress cycles. The geometry function,  $Y(a)$ , for specific cracked component and loading conditions may be obtained from the available stress intensity manuals or derived using fracture mechanics principles.

The geometry function depends on the geometry of the cracked body (e.g., plate, pipe), crack size, crack location (e.g., edge, center, distributed) and loading (e.g., normal load, bending).

To account for the variable amplitude stress ranges that result from random stress range,  $\Delta\sigma$  can be replaced by an effective constant stress range,  $\Delta\sigma_{eff}$ , which represents a weighted effect of stress ranges of all amplitudes and produces the same crack growth rate. The effective stress range,  $\Delta\sigma_{eff}$ , can be expressed in terms of gamma function,  $\Gamma( )$ , (Chung et al., 2006) as follows:

$$\Delta\sigma_{eff} = \left( E[\Delta\sigma^m] \right)^{\frac{1}{m}} \quad (5.4)$$

where  $E[\Delta\sigma^m]$  is mean of  $\Delta\sigma^m$ .

For Weibull distribution,  $E[\Delta\sigma^m]$  can be calculated as follows (Cramer et al., 1992):

$$E[\Delta\sigma^m] = \theta^m \cdot \Gamma(1 + \frac{m}{\beta}) \quad (5.5)$$

where  $\theta$  and  $\beta$  are scale and shape parameter of Weibull distribution, respectively.

Analytical integration of Paris Law is not possible in most applications since the geometry functions are not mathematically simple. In this case the integration cycle by cycle method may be applied, see Yee (1997). For simplicity consider the case of a loaded component where  $Y(a)$  does not change much within the range of  $a_0$  to the critical size,  $a_{cr}$ , an average geometry function,  $Y_{av} = [Y(a_0) + Y(a_{cr})]/2$  may be used; hence integration of Paris Law yields (Ragab and Bayoumi, 1999):

For  $m = 2$ :

$$N_{cr} = \frac{\ln(a_{cr}/a_0)}{C\pi(\Delta\sigma_{eff} \cdot Y_{av}(a))^2} \quad (5.6)$$

For  $m \neq 2$ :

$$N_{cr} = \frac{a_{cr}^{(1-\frac{m}{2})} - a_o^{(1-\frac{m}{2})}}{C(Y_{av})^{\frac{m}{2}} (\Delta\sigma_{eff})^m (1-m/2)} \quad (5.7)$$

where  $N_{cr}$  is the critical number of stress cycles and  $a_{cr}$  is the critical crack size.

Substituting  $N_{cr} = f \cdot t_{cr}$  where  $f$  is frequency of loading (e.g. 500,000 cycle/year) and  $t_{cr}$  is the critical time to failure. This leads to the critical time to failure as follows:

For  $m = 2$ :

$$t_{cr} = \frac{\ln(a_{cr}/a_o)}{f \cdot C \cdot \pi \left( \left( E[\Delta\sigma^n] \right)^{\frac{1}{m}} \cdot Y_{av} \right)^2} \quad (5.8)$$

For  $m \neq 2$ :

$$t_{cr} = \frac{a_{cr}^{(1-\frac{m}{2})} - a_o^{(1-\frac{m}{2})}}{f \cdot C \cdot [Y_{av}]^{\frac{m}{2}} \cdot E[\Delta\sigma^n] \cdot [1-m/2]} \quad (5.9)$$

The crack size can be obtained as a function of time as follows:

For  $m = 2$ :

$$a(t) = a_o \cdot \text{Exp} \left( t \cdot f \cdot C \cdot \pi \left( \left( E[\Delta\sigma^n] \right)^{\frac{1}{m}} \cdot Y_{av} \right)^2 \right) \quad (5.10)$$

For  $m \neq 2$ :

$$a(t) = \left( t.f.C.(Y_{\sigma^t})^{\frac{m}{2}}.E[\Delta\sigma^m].(1-m/2) + a_o^{(1-m/2)} \right)^{1/(1-m/2)} \quad (5.11)$$

Corrosion produces material flaws such as metal loss, pitting, cracks or/and degradation of material properties due to changes in the material microstructure. If a flaw is not acceptable according to specified criteria, it is referred to as a defect. We here use the term flaw as we are interested in estimating the flaw size even before it becomes a defect.

The flaw is propagated by corrosive effects until the critical size, such that failure occurs. The historical data of the corrosion inspections can be used to determine the corrosion rate and the corrosion flaw size at a specific time. For example, the growth of the pit depth,  $a_p$ , can be modeled using a power law as follows:

$$a_p = a_o + c t^b \quad (5.12)$$

where  $c$  and  $b$  are constants. Values of  $b$  for pitting corrosion ranges from 0.33 to 0.6 (Laycock et al., 1999). The pitting rate at any time  $t$  is determined as the slope of the tangent of the curve of  $a_p$  as a function of  $t$ . The value of  $b$  is sometimes

conservatively assumed 1 since values of b less than 1 result in decreasing pitting rates with time.

For the types of corrosion which produce cracking such as stress corrosion cracking (SCC) or hydrogen induced cracking (HIC), experimental data relating the crack growth rate ( $da/dt$ ) to the stress intensity factor, K, can be obtained. The best fit to crack growth data generated under operating conditions and environments is obtained and usually is described using a power law of the form:

$$\frac{da}{dt} = \eta \cdot (K - K_{th})^\gamma \quad (5.13)$$

where

$\eta$  and  $\gamma$  are empirical constants dependent on the material condition, temperature and environment.

K is the crack tip stress intensity factor.

$K_{th}$  is the crack tip stress intensity factor threshold for the specified corrosion cracking mechanism such as stress corrosion cracking, SCC.

The proposed methodology focused on two specific degradation mechanisms: fatigue and corrosion. The methodology can be extended to other types of degradation mechanisms including the interaction of two or more degradation

mechanisms at same time such as corrosion-fatigue-creep interaction. In order to extend this methodology to other degradation mechanisms, an accurate fracture mechanics model is to be used to estimate the flaw size (damage size due to these degradation mechanisms) at any time,  $t$ .

### 5.2.3 Inspection and maintenance planning

Inspections are usually scheduled at specified intervals. The inspection intervals may be fixed, variable over the life time, or a fraction of the remaining life. For example, according to the recommendations of API 570 (1998) the inspection of pipelines is carried out at intervals selected on the basis of a qualitative judgement by the expert but not allowed to exceed half of the remaining life.

In the proposed work, the inspection interval is selected as a fraction,  $R$ , of the remaining life.  $R$  is a controllable (decision) variable in the optimization problem and is determined on the basis of the optimization of the RBIM plan. Figure 5-2 shows the inspection intervals between the initial time,  $t_0$ , and the critical time to failure,  $t_{cr}$  as a fraction of the remaining life. It should be noted that the inspection intervals decrease with the decrease in the remaining life (the period from the inspection time  $t_i$  to the critical time,  $t_{cr}$ ). This inspection strategy allows more inspections of the asset as it approaches the critical time to failure.

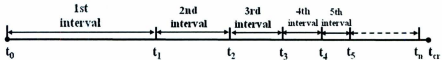


**Figure 5-2:** Inspection intervals as a fraction of the remaining life.

The condition of the inspected asset dictates the maintenance action that needs to be taken. The asset may be repaired, replaced, or left as is depending on its condition. The action taken is based on the maintenance cost and the acceptable risk of failure of the asset to perform its intended function until the next inspection. A balance between the cost of inspection and maintenance and risk of failure is achieved to optimize the RBIM plan.

#### 5.2.4 Risk assessment

Risk is expressed as the product of two factors: probability of failure and the consequences of failure.

##### 5.2.4.1. Probability of failure

The probability of failure,  $P_f$ , is defined as probability of non-detecting a growing flaw before reaching the critical time to failure,  $t_{cr}$ . It is estimated as follows (Chung et al., 2006):

$$P_f = \frac{\sum_{j=1}^S \left[ \prod_{i=1}^{N_j} (1 - POD(a_i)) \right]}{S} \quad (5.14)$$

where S is number of simulations. N<sub>j</sub> is number of inspections before reaching the critical time to failure, t<sub>cr</sub> in the jth simulation. POD(a<sub>i</sub>) is probability of detection of a flaw with size a<sub>i</sub> in the ith inspection.

#### *5.2.4.2. Consequences of failure*

The failure could lead to physical injury to personnel in the vicinity and cause structural damage to surrounding equipment. In addition it could lead to release of the contaminants. The release could be flammable, toxic, high pressure or hot fluid releases. The subsequent consequences resulting from the release depend on the type of fluid and the energy contained in the system. These consequences could make business interruption, damage to equipments, people, and/or environment. Modeling of the releases and dispersion in process units can be found in Crowl and Lowar (2002).

The cost of failure consequences is multiplied by the probability of failure to estimate the risk as follows:

$$R_F = P_f \cdot k_F \quad (5.15)$$

where  $k_F$  is cost of failure consequences.

From Eqs. 5.14 and 5.15, the risk of failure is given by:

$$R_f = \frac{\sum_{j=1}^S \left[ \prod_{i=1}^{N_j} (1 - POD(a_i)) K_F \right]}{S} \quad (5.16)$$

### 5.2.5 The expected cost of inspections over the lifetime

The number of inspections between  $t_0$  and  $t_{cr}$  is estimated based on the strategy shown in Figure 5-2. Since  $t_{cr}$  is a function of the material parameters, operating and environmental conditions, and the initial flaw size ( $a_0$ ). In general these are random variables. Monte Carlo simulation is used to account for all possible combinations of these random variables. The expected number of inspections,  $N_{ins}$ , is estimated as the average of number of inspections estimated in each simulation as follows:

$$N_{ins} = \frac{\sum_{j=1}^S N_j}{S} \quad (5.17)$$

Figure 5.3 shows two different simulations of the flaw size growth with time.

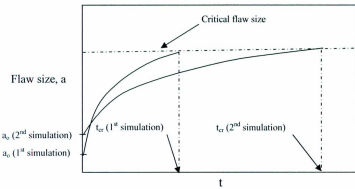


**Figure 5-3:** Simulation of the flaw size growth with time (after Chung et al., 2006).

The expected cost of inspections,  $C_I$ , over the lifetime is estimated as follows:

$$C_I = N_{ins} \cdot n \cdot k_I \quad (5.18)$$

where  $n$  is sample size and  $k_I$  is the cost of one inspection. When inspection and maintenance are planned for only one component; then, sample size,  $n = 1$ . However for a complete system or asset, it is often required to inspect a sample representative to the entire system/asset.

From Eqs. 5.17 and 5.18, the expected cost of inspections over the lifetime is given by:

$$C_r = \frac{\sum_{j=1}^S N_j n k_j}{S} \quad (5.19)$$

### 5.2.6 The expected cost of repairs over the lifetime

A repair will be undertaken if the detected crack is larger than the maximum acceptable crack size,  $a_r$ . Let  $A(a_i) = \text{probability of acceptance of crack with size } a_i \text{ at the } i\text{th inspection} = P(a_i < a_r)$ . The probability of repair at the  $i$ th inspection is estimated as follows:

$$P_r(a_i) = POD(a_i) \cdot (1 - A(a_i)) \quad (5.20)$$

where  $A(a_i) = 1$  if  $a_i \leq a_r$  and  $A(a_i) = 0$  if  $a_i > a_r$ .

The cost of repair,  $C_r$ , for each simulation of the flaw growth is estimated as follows:

$$c_r = \sum_{i=1}^{N_f} [P_r(a_i) n k_R] \quad (5.21)$$

where  $k_R$  is cost of one repair.

The expected cost of repairs,  $C_R$ , over the lifetime is estimated as the average repair cost from all simulations as follows:

$$C_R = \frac{\sum_{j=1}^S C_r}{S} = \frac{\sum_{j=1}^S \sum_{i=1}^{N_j} [POD(a_i).(\mathbb{I} - A(a_i)).n k_g]}{S} \quad (5.22)$$

### 5.2.7 Optimization of the inspection intervals

The objective function, OF, is defined as the summation of the inspection cost, repair cost and risk of failure as follows:

$$OF = C_I + C_{Rep} + C_R + R_F - R_V \quad (5.23)$$

where  $C_{Rep}$  is the replacement cost.  $R_V$  is the remaining value of the asset or the system after a defined period T (study period).

Since the remaining life is different when using different maintenance options (repair or replacement), the remaining value after period of time, T, is considered as a benefit for a maintenance option leading to a remaining life greater than T. This is similar to what is carried out in cost/benefits analysis.

All costs in the objective function at different points of time are to be discounted to a present value when comparing different inspection and maintenance plans. The net present values, NPV of the cost of inspection, cost of repair and risk of failure are given as follows:

$$NPV(C_t) = \frac{\sum_{j=1}^S \left[ \sum_{i=1}^{N_j} \frac{n_k}{(1+r)^{t_i}} \right]}{S} \quad (5.24)$$

$$NPV(C_R) = \frac{\sum_{j=1}^S \sum_{i=1}^{N_j} \left[ POD(a_i) \cdot (1 - A(a_i)) \cdot \frac{n_k}{(1+r)^{t_i}} \right]}{S} \quad (5.25)$$

$$NPV(R_r) = \frac{\sum_{j=1}^S \left[ \prod_{i=1}^{N_j} (1 - POD(a_i)) \cdot \frac{n_k}{(1+r)^{t_i}} \right]}{S} \quad (5.26)$$

where r is the discount rate and  $t_i$  is time of the ith inspection.

The net present values of  $C_{Repl}$  and  $R_V$  are obtained as follows:

$$NPV(C_{Repl}) = \sum \frac{C_{Repl}}{(1+r)^{t_{Repl}}} \quad (5.27)$$

where  $t_{Repl}$  is time of replacement. It should be noticed that a maintenance option could include replacement many times during the lifetime.

$$NPV(R_r) = \frac{R_r}{(1+r)^T} \quad (5.28)$$

The net present value of the objective function, NPV(OF), can be estimated as:

$$NPV(OF) = NPV(C_i) + NPV(C_{Re,p}) + NPV(C_R) + NPV(R_F) - NPV(R_v) \quad (5.29)$$

The future annual costs of labour and materials tend to increase in future. An escalation rate may be used to predict inspection cost ( $k_i$ ), repair cost ( $K_R$ ) and failure cost ( $K_F$ ) at different points of time.

The inspection intervals are selected as a fraction,  $R$ , of the remaining life (Figure 5-2). Figure 5-4 shows the cost (inspection and maintenance), risk of failure and the objective function for different values of the ratio,  $R$ . The costs of inspection and repair decrease as  $R$  increases because the smaller  $R$  the greater the expected number of inspections and repairs during the lifetime will be. As  $R$  increases, the risk of failure increases. The objective function is then estimated for different values of  $R$  as the sum of inspection cost (decreasing curve), repair cost (decreasing curve), replacement cost (constant), risk of failure (increasing curve) and remaining value (constant). The resultant objective function has a concave form (Figure 5-4). The optimum inspection interval is obtained using an  $R$  value determined by the minimum value of the objective function provided that the risk of failure does not exceed the pre-defined level.

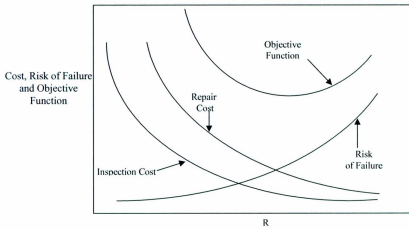


**Figure 5-4:** Cost (inspection and repair), risk of failure and objective function versus different values of R for a suggested inspection and maintenance plan.

The solution of the optimization problem is repeated for different suggested inspection and maintenance plans and the minimum values of the objective function are compared to select the optimum inspection and maintenance plan.

### 5.3 Case study No. 1

A welding joint located in a 50 m free span of 20" subsea pipeline subjected to fatigue due to vortex induced vibrations (VIV) is considered in this case study. As the RBIM plan is carried out for only one component, the sample size,  $n=1$ .

The distribution of the stress range ( $\Delta\sigma$ ) is modeled by Weibull distribution (Tronsker et al., 2002) with a cumulative probability density function given by:

$$F(\Delta\sigma) = 1 - \exp\left[-\left(\frac{\Delta\sigma}{\theta}\right)^\beta\right] \quad (5.30)$$

where  $\theta$  (scale parameter) = 13.4 Mpa and  $\beta$  (shape parameter) = 1.5.

The average number of stress cycles per year (frequency) is  $2.4 \times 10^6$  cycle/year. The critical crack size (depth of the crack at which leakage will occur),  $a_{cr}$  is considered as 5 mm for this case study.

The fatigue crack growth parameter, C, is modeled as a lognormally distributed random variable with a mean value of  $6.06 \times 10^{-13}$  assuming units of millimeters for crack size and MPa.mm<sup>1/2</sup> for stress intensity factor, K, and a standard deviation of  $1.58 \times 10^{-13}$  mm. The fatigue crack growth exponent, m, is modeled as a normally distributed random variable with a mean value of 3 and a standard deviation of 0.14 mm (Chung et al., 2006).

The costs of inspection ( $K_I$ ), repair ( $K_R$ ) and failure consequences ( $K_F$ ) are taken as  $\$10^2$ ,  $\$10^3$  and  $\$10^5$ , respectively.

The optimization problem is subject to two constraints that the maximum acceptable risk of failure is \$5000 and the minimum inspection interval is 1 year.

Ultrasonic inspection (UI) technique is considered. The POD functions for the Ultrasonic inspection technique based on data obtained from test results of a flat plate collected by Berens and Hovey (1981) are modeled as follows:

$$POD(a) = \frac{\exp(A + B \cdot \ln a)}{1 + \exp(A + B \cdot \ln a)} \quad (5.31)$$

where A and B are parameters obtained experimentally as -0.119 and 2.986, respectively.

The repair policy dedicates the repair for any detected crack size larger than 50% of the critical size (i.e.  $a_r = 0.5a_{cr}$ ). The minimum inspection interval is 1 year. The geometry function, Y, is taken as a constant and equal to unity for simplicity in this case study.

The following two inspection and maintenance plans are compared:

Plan A: Inspection using ultrasonic inspection (UI) technique. The initial crack size,  $a_0$ , is modeled as a lognormally distributed random variable with a mean value of 2 mm and a standard deviation of 1 mm. The remaining value of the welding joint after a study period of 20 years is assumed \$0.

Plan B: Replacement of the welding joint and schedule a follow up inspection using ultrasonic inspection (UI) technique. The cost of replacement is

\$10000. The initial crack size,  $a_0$ , is modeled for the new joint as a lognormally distributed random variable with a mean value of 1 mm and a standard deviation of 0.5 mm. The remaining value of the welding joint after a study period of 20 years is assumed \$1000.

All costs of inspection, repair and failure consequences are reduced to a present value with a reduction ratio,  $r$ , of 10%.

Since the stress range,  $\Delta\sigma$ , is modelled by Weibull distribution, the  $E[\Delta\sigma_m]$  is estimated using Eq. 5.5. The crack size as a function of time is obtained from Eq. 5.5 and Eq. 5.11 as follows:

$$a(t) = \left( t.f.C(Y_{av})^m \pi^{m/2} \theta^m \Gamma(1 + \frac{m}{\beta}) (1 - m/2) + a_0^{(1-m/2)} \right)^{1/(1-m/2)} \quad (5.32)$$

Monte Carlo is used to generate large random sets of the random variables ( $a_0$ , C and m). Each set of random ( $a_0$ , C and m) is used in Eq. 5.9 to estimate a value of the critical time to failure,  $t_{cr}$ , (corresponding to  $a_{cr}$ ). The expected (mean) critical time to failure is obtained as the average of the critical time to failure from all simulations.

Plan A: The critical time to failure is estimated as 21 years. The net present values of inspection cost, repair cost and risk of failure are estimated using Eqs.

5.24, 5.25 and 5.26 for different values of the ratio R as shown in Figures 5-5 and 5-6.

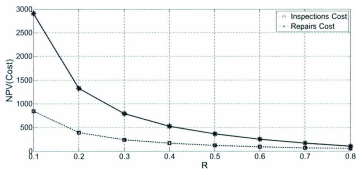


**Figure 5-5:** The net present values of the cost (inspections cost and repairs cost) for different values of R (plan A).

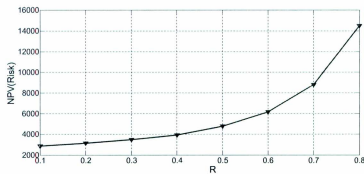


**Figure 5-6:** The net present values of risk of failure for different values of R (plan A).

The net present value of the objective function,  $NPV(OF)$ , is obtained using Eq. 5.29 as shown in Figure 5-7.

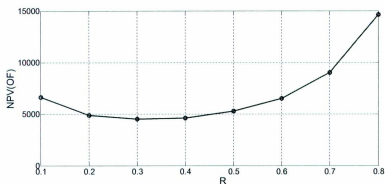


**Figure 5-7:** The net present value of the objective function for different values of  $R$  (plan A).

The minimum  $NPV$  of the objective function is \$4515 corresponds to  $R = 0.3$  (Figure 5-7). At  $R = 0.3$ , the expected  $NPV$  of the inspection cost over the expected lifetime (21 years) is \$241.43 (Figure 5-5), the expected  $NPV$  of the repair cost over the expected lifetime is \$794.1 (Figure 5-5) and the expected  $NPV$  of the risk of failure is \$3450 (Figure 5-6). The risk constraint is fulfilled as the expected  $NPV$  of the risk of failure at  $R = 0.3$  is less than the maximum acceptable risk of failure (\$5000). Hence, the optimum ratio  $R$  for plan A is 0.3 of the

remaining life corresponding to the following optimum inspection schedule (Table 5-1):

**Table 5-1:** The optimum inspection schedule for plan A (case study No. 1).

Inspection no.	Time, year	Inspection interval, year	Remaining life, year
---	0	---	21
1	6.30	6.30	14.70
2	10.71	4.41	10.29
3	13.80	3.09	7.20
4	15.96	2.16	5.04
5	17.47	1.51	3.53
6	18.53	1.06	2.47

Plan B: The critical time to failure is obtained as 41 years. The net present values of inspection cost, repair cost and risk of failure for different values of R are shown in Figures 5-8 and 5-9.

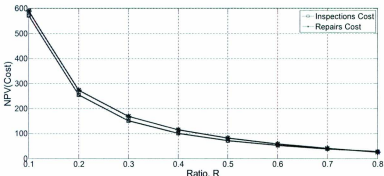


**Figure 5-8:** The net present value (NPV) of the cost (inspections cost and repairs cost) for different values of the ratio R (plan B).

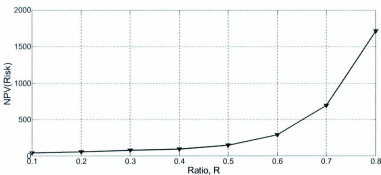


**Figure 5-9:** The net present value (NPV) of the risk of failure for different values of the ratio R (plan B).

The net present remaining value after a period,  $T = 20$  years is estimated using Eq. 5.28 as \$148.64. The net present value of the replacement cost equals

the replacement cost (\$10000) as it is paid one time at time  $t_0 = 0$ . The net present value of the objective function,  $NPV(OF)$ , is estimated for different values of  $R$  as shown in Figure 5-10.

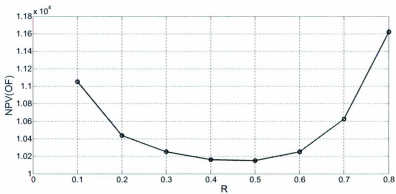


**Figure 5-10:** The net present value (NPV) of the objective function for different values of the ratio  $R$  (plan B).

The minimum NPV of the objective function is \$10150 corresponds to  $R = 0.5$  (Figure 5-10). At this ratio, the expected NPV of the inspection cost over the expected lifetime (41 years) is \$71.36 (Figure 5-8), the expected NPV of the repair cost over the expected lifetime is \$81.24 (Figure 5-8) and the expected NPV of the risk of failure is \$146.04 (Figure 5-9).

The risk constraint is fulfilled as the expected NPV of the risk of failure at  $R = 0.5$  is less than the maximum acceptable risk of failure (\$5000). Hence, the

optimum ratio R for plan B is 0.5 of the remaining life corresponding to the following optimum inspection schedule (Table 5-2):

**Table 5-2:** The optimum inspection schedule for plan B (case study No. 1).

Inspection no.	Time, year	Inspection interval, year	Remaining life, year
---	0	--	41
1	20.5	20.5	20.5
2	30.75	10.25	10.25
3	35.88	5.13	5.13
4	38.44	2.56	2.56
5	39.72	1.28	1.28

Plan A requires to schedule 6 follow up inspections of the existing welding joint (Table 5-1) while plan B requires to replace the welding joint and schedule 5 follow up inspections for the new joint (Table 5-2). Since the optimum NPV(OF) for plan A (\$4515 at  $R = 0.3$ ) is less than the optimum NPV(OF) for plan B (\$9967 at  $R = 0.5$ ), plan A is the optimum inspection and maintenance plan.

The cost of failure consequences,  $K_F$  is increased to  $10^7$  instead of  $10^5$  while keeping all other parameters without change to check the effect of any change in failure cost on deciding the optimum plan. In this case, the optimum RBIM plan is plan B with optimum inspection interval equals to a ratio  $R = 0.2$  of the remaining life (Figure 5-11). The selection of the optimum plan is changed and the inspection interval is decreased as a result of increasing the failure cost.

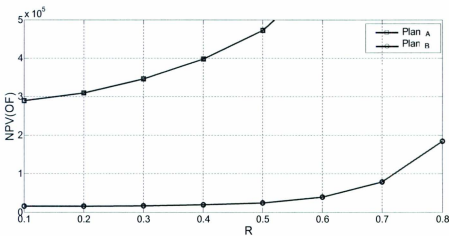


**Figure 5-11:** The effect of failure cost ( $K_F=10^7$ ) on the optimal selection of RBIM plan.

#### 5.4 Case study No. 2

Consider a process pipeline subjected to pitting corrosion. The pit growth rate is modeled by Eq. 5-12 with  $c = 0.237$  mm and  $b = 0.35$ . The initial pit depth,  $a_0$ , is modeled as a random variable following Gumbel distribution with location parameter 0.91 mm and scale parameter 0.156 mm. The critical pit size (depth of the pit at which leakage will occur),  $a_{cr}$  is considered as 0.75 of the nominal thickness (9.5 mm). For assessing pipelines containing corrosion, see DNV-RP-F101 (2004).

The expected remaining life is obtained using the simulation of  $a_o$  in Eq. 5-12 as 16.62 years. The study period, T, is taken equal to the expected remaining life.

The costs of inspection ( $K_I$ ), repair ( $K_R$ ) and failure consequences ( $K_F$ ) are taken as  $\$10^2$ ,  $\$10^3$  and  $\$10^6$ , respectively. Assume the pipeline is divided into 100 segments (sample size is n=100).

The optimization problem is subject to two constraints that the maximum acceptable risk of failure is \$5000 and the minimum inspection interval is 1 year.

Ultrasonic inspection (UI) technique is considered. The POD function of UI technique for pitting corrosion is assumed the same as obtained from test results of a flat plate collected by Berens and Hovey (1981), Eq. 5.31 for illustration in this case study. It should be noted that, in practical applications, POD function should be obtained for a specific application as POD is sensitive to type of the flaw, material and geometry of the flawed body (Chung et al., 2006).

The repair policy dedicates the repair for any detected crack size larger than 50% of the critical size (i.e.  $a_r = 0.5a_{cr}$ ). The minimum inspection interval is 1 year.

All costs (inspection, repair and failure consequences) are reduced to a present value with a reduction ratio, r, of 10%.

The net present values of inspection cost, repair cost and risk of failure are estimated using Eqs. 5.24, 5.25 and 5.26 for different values of R as shown in Figures 5-12 and 5-13.

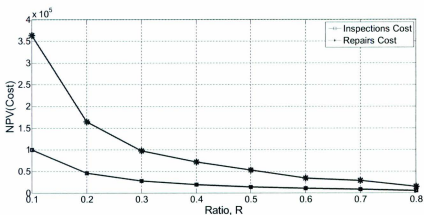


**Figure 5-12:** The net present values of the cost (inspections cost and repairs cost) for different values of R.

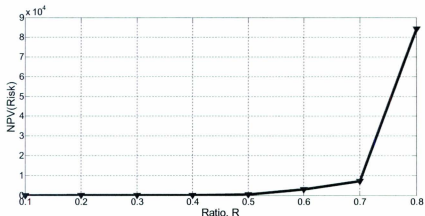


**Figure 5-13:** The net present values of risk of failure for different values of R.

The net present value of the objective function, NPV(OF), is obtained using Eq. 5.29 as shown in Figure 5-14.

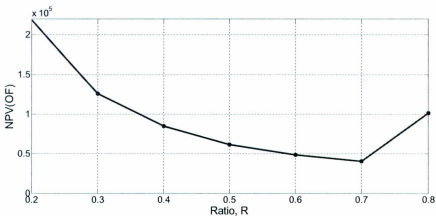


**Figure 5-14:** The net present value (NPV) of the objective function for different values of the ratio R.

The minimum value of the objective function is  $\$4.03 \times 10^4$  corresponding to  $R = 0.7$ . The risk of failure at  $R = 0.7$  is greater than the acceptable risk (\$5000), see Figure 5-13; thus, the optimum R is reduced to 0.5 to satisfy this risk constraint. The optimum inspection schedule is shown in Table 5-3.

**Table 5-3:** The optimum inspection schedule (case study No. 2).

Inspection no.	Time, year	Inspection interval, year	Remaining life, year
---	0	--	16.62
1	8.31	8.31	8.31
2	12.46	4.16	4.16
3	14.54	2.08	2.08
4	15.58	1.04	1.04

## **5.5 Conclusion**

A quantitative risk-based inspection and maintenance (RBIM) methodology is proposed for inspection and maintenance planning, in a cost effective way that helps in maintaining the integrity of process assets.

The proposed methodology is comprised of the following main steps: classification of the asset's components/areas according to criticality of deterioration, asset deterioration modeling, risk assessment, cost estimation (inspection and maintenance costs over the expected lifetime), and the optimal selection of inspection schedule and maintenance action.

The proposed methodology allows the minimization of the cost of inspection and maintenance over the lifetime of a deteriorated asset/system without compromising the safety.

The details of the proposed methodology are illustrated through two case studies of a welding joint subjected to fatigue and a pipeline subjected to pitting corrosion.

## **CHAPTER 6**

### **Conclusion and Future Work**

#### **6.1. Conclusion**

In this thesis, a framework is developed for optimal risk RBIM planning for process components subjected to fatigue and corrosion. This framework includes two main parts:

- Inspection sampling: This part estimates the required inspection sample size for process assets subjected to general corrosion and localized corrosion such as stress corrosion cracking, hydrogen induced cracking and pitting corrosion.
- Optimization of the risk-based inspection and maintenance (RBIM) plan: This determines the optimal inspection intervals and maintenance activities required to maintain asset integrity in a cost effective way.

In the case of general corrosion, the aim of the inspection is to investigate the mean metal loss. A closed-form formula has been introduced to estimate the sample size required to assess the mean metal loss of process components due to

general corrosion. The closed-form formula uses Bayesian theory to update prior information based on newly obtained information. The sample size is estimated to guarantee an acceptable margin of error in the estimate of the mean metal loss at a given confidence level. The effect of population size and prior knowledge on the determination of sample size is discussed. The proposed approach to determine sample size minimizes the required sample size that needed to assess general corrosion based on the past history and new inspection data.

Failure due to localized corrosion could occur at the location of the maximum corrosion size. Thus, the aim of the inspection of localized corrosion is to investigate the maximum corrosion size. A methodology has been proposed for calculating the sample size required for the inspection of localized corrosion. The proposed methodology consists of: i) layering separation, ii) physical sampling, ii) bootstrap sampling and extreme value analysis, and iv) estimation of sample size. The estimated sample size ensures an acceptable precision in the prediction of the maximum localized corrosion over the entire population. The precision is assessed based on the predicted maximum localized corrosion, using the extreme value method, is within a pre-defined margin of error at a specified confidence level. A formula is developed to estimate sample size based on the proposed methodology.

The extreme value method and the Bayesian updating approach are integrated in a single proposed algorithm to estimate the sample size required to assess localized corrosion of process components. Using this algorithm, two closed-form formulas for calculating sample size for the inspection of localized corrosion have been proposed. The first formula addresses the situation when prior information is available from past inspections. In this situation, the calculated sample size is based on combining newly obtained information and prior information using Bayesian probability theory. The second formula addresses the situation when prior information is not available.

The optimization problem of risk-based inspection and maintenance (RBIM) planning is based on minimizing an objective function. The objective function is formulated as the sum of the costs of inspection and maintenance (repair/replacement) over the asset's lifetime, risk of failure and the remaining value of the asset after a specified period of time. The controllable factors in the optimization problem are the inspection interval, inspection technique and the maintenance action (repair/replacement). The selection of these factors is based on minimizing the objective function and therefore produces an optimized RBIM plan.

The expected cost of inspection is estimated as multiplication of the expected number of inspections over the lifetime, the sample size and the cost of one inspection.

Repair is undertaken if the detected flaw is larger than the acceptable value of the flaw size. The probability of repair at the  $i$ th inspection is estimated as the probability of detection of a flaw of unacceptable size. The cost of repair is evaluated as the sum- over all inspections during the asset's lifetime- of the product of the probability of repair at time of the  $i$ th inspection, the sample size and the cost of each repair. The probability of failure,  $P_f$ , is defined as the probability of non-detecting a growing flaw before reaching the critical time to failure. The risk of failure is estimated as the product of the probability of failure and the failure consequences.

The inspection interval is selected as a fraction,  $R$ , of the remaining life. This inspection strategy allows more inspections of the asset as it approaches the critical time to failure. An inspection plan involves the selection of an inspection technique and schedule. A maintenance plan involves making decisions regarding the maintenance activity (repair/replacement) to be performed. To solve the optimization problem, an appropriate inspection interval (as a fraction,  $R$ , of the remaining life), inspection technique and maintenance activity

(repair/replacement) are suggested. The net present value of the objective function is estimated for different values of R. The cost of inspections and repairs over the assets's lifetime give a decreasing function of R, while the risk of failure gives an increasing function of R. The resulting objective function has a concave form. The optimum interval schedule for suggested inspection technique and maintenance action is obtained by determining the value of R, which minimizes the objective function subject to two main constraints: i) the risk of failure does not exceed an acceptable limit ii) the inspection interval is larger than a pre-defined threshold. The second constraint is used to ensure that the inspection strategy will not cause unnecessary interruptions during operations. Other constraints such as the size of the maintenance budget may also be applied. The optimization problem is solved for different suggested inspection techniques and maintenance actions, and the minimum values of the objective are compared to obtain the optimum RBIM plan.

## **6.2. Significance and originality of the thesis**

This thesis presents a breakthrough in solving the problem of inspection sampling and RBIM for process components. Important tools and methods have been used such as the bootstrap sampling, Monte-Carlo simulation, extreme value method and Bayesian updating method. The results obtained using the

methodology for inspection sampling of localized corrosion provide new closed-form formulas to calculate sample size.

Integrating the Bayesian updating method with the extreme value method in one algorithm to estimate sample size of localized corrosion is a unique effort. This algorithm is an original contribution which will help to minimize the required sample size to assess localized corrosion.

The developed model for RBIM planning helps to decide the optimum inspection technique and inspection interval as a fraction of the remaining life of the asset. This model also assists in making optimum decisions regarding the optimum maintenance activity such as repair or replacement based on minimizing the objective function while keeping the risk level within the acceptable limit.

This work has combined a variety of methods into a single quantitative framework to help operators in making well informed decisions to plan inspection and maintenance activities in a cost effective way without compromising the required level of safety.

### **6.3. Future work**

- a) A methodology for risk-based inspection sampling (RBIS) will be introduced. This methodology will aim to estimate the required sample size

to assess deteriorated assets due to different damage mechanisms based on a non-classical concept. Within this concept, the estimated sample size should ensure that the risk of failure of both inspected and non inspected components/areas does not exceed a pre-defined limit.

- b) Physical failure modeling was used in the introduced methodology for optimal RBIM planning. This methodology is useful for fixed equipment such as pipelines, vessels, heaters towers and heat exchangers subjected to damage mechanisms, such as fatigue and corrosion. A different methodology is required for rotary equipment such as pumps, compressors and turbines in which failure occurs randomly due to a variety of reasons such as mechanical seal failure, bearing failure, shaft misalignment and incorrect installation. Statistical failure modeling is a better approach for this type of failure. This methodology will be used for making inspection and maintenance decisions for rotary equipments.
- c) A software program will be developed based on the overall framework provided in this thesis to estimate sample size and optimize the inspection and maintenance plan.

## **References**

- Adcock, C. J. (1988). A bayesian approach to calculating sample sizes. *The Statistician*. 37, 5, 433-439.
- Agarwal, H., Renaud, E. J., Preston, L.E. and Padmanabhan, D. (2004). Uncertainty quantification using evidence theory in multidisciplinary design optimization. *Reliability Engineering and System Safety*, Elsevier Ltd. 85, 281-294.
- Ahmadi A., and Kumar U. (2011). Developed a cost based risk model to identify inspection and restoration intervals of hidden failures subject to aging. *IEEE Transactions on Reliability*. 60, 197-209.
- Alfonso, L., Caleyo, F., Hallen, J.M., Esplna-Hernandez J.H. and Escamilla-Davish, J.J. (2008). Application of extreme value statistics to the prediction of maximum pit depth in non-pigable, buried pipelines. *Proceedings of IPC2008 7th International Pipeline Conference*, Calgary, Alberta, Canada.
- Ang, A. and Tang, W. (2007). *Probability Concepts in Engineering*, (2nd Ed.). New York: John Wiley and Sons.
- Apeland, S. and Aven T. (1999). Risk based maintenance optimization: foundational issues. *Reliability Engineering and System Safety*. 67, 285-292.

API 510 (1998). Pressure Vessels Inspection Code. Washington, D.C: American Petroleum Institute.

API 570 (1998). Inspection, Repair, Alteration and Rerating of In-Service Piping Systems. Washington, D.C: American Petroleum Institute.

API 581 (2000). Risk-based inspection: Base resource document. Washington, D.C: American Petroleum Institute.

ASME (1991). Risk-Based Inspection-Development of Guidelines. American Society of Mechanical Engineers (ASME), New York.

ASME (1999). Risk Based Inspection (RBI): A Risk-based approach to planned plant inspection. Health and Safety Executive – Hazardous Installations Division, CC/TECH/SAFETY/8.

ASME B31G (2009). Manual for determining the remaining strength of corroded pipelines. The American Society of Mechanical Engineers, New York.

ASME Boiler and Pressure Vessel Code, section XI (2004). Rules for inservice inspection of nuclear power plant components. New York, N.Y: American Society of Mechanical Engineers.

ASTM E122 (2009). Standard practice for calculating sample size to estimate, with specified precision, the average for a characteristic of a lot or process.

ASTM G46-94 (2005). Standard Guide for Examination and Evaluation of Pitting Corrosion.

Ayyub, B. and Klir, J. G. (2006). Uncertainty Modeling and Analysis in Engineering and the Sciences. Published by Chapman & Hall/CRC.

Balkey, K., Art, R.. and Bosnk, R. (1998). ASME Risk-Based in service inspection and testing: an outlook to the future. Society for risk analysis. 18, 407-421.

Baraldi, P. and Zio, E. (2008). A Combined Monte Carlo and Possibilistic Approach to Uncertainty Propagation in Event Tree Analysis. Risk Analysis. 28, 4, 1-17.

Berens, A.P. and Hovey, P.W. (1981). Evaluation of NDE Reliability Characterization. AFWAL-TR-81-4160, 1, Air Force Wright-Aeronautical Laboratory, Wright-Patterson Air Force Base, Dayton, Ohio.

Bernstein, S. and Bernstein, R. (1999). Schaum's outline of theory and problems of elements of statistics II: Inferential statistics. New York: McGraw-Hill.

Brooker, D.C. and Geoffery K.C. (2004). Accurate calculation of confidence intervals on predicted extreme met-ocean conditions when using small data sets. Proceeding of the 23<sup>rd</sup> International Conference on Offshore Mechanics and Arctic Engineering (OMAE). 2, 149-154.

Chung, Hsin-Yang, Manuel, L. and Frank, K.H. (2006). Optimal Inspection Scheduling of Steel Bridges Using Non Destructive Testing Techniques. Journal of Bridge Engineering. 11, 305-319.

Cohen, M.P. (1997). Bayesian bootstrap for unequal probability sample designs for application to multiple imputation. National Center for Education Statistics, 555 New Jersey Avenue NW, Washington DC 20208-5654.

Cramer, E.H. and Friis-Hansen, P., (1992). Reliability Based Optimization of Multi-Component Welded Structures. OMAE, II, Safety and Reliability ASME 1992, Proceeding Of The 11th International Conference on Offshore Mechanics And Arctic Engineering, Calgary, Canada. 2, 265-271.

Crowl, D. A. and Lowar, J. F. (2002). Chemical Process Safety: Fundamentals with Applications (2nd Edition). Prentice Hall, Inc., Upper Saddle River, NJ 07458.

De Santis, F. (2007). Using historical data for bayesian sample size determination. *Journal of the Royal Statistical Society: Series A (Statistics in Society)*, 170(1), 95-113.

DNV-RP-F101 (2004). Corroded pipelines: DNV recommended practice. Hovik, Norway: Det Norske Veritas.

Druschel, R.B., Ozbek, M. and Pinder, G. (2006). Application of Dempster-Shafer theory to hydraulic conductivity. CMWR – XVI, Conference Program, Copenhagen, Denmark. 5, 31-33.

Ebeling, E.C. (1997). An Introduction to Reliability and Maintainability Engineering. (1st Ed). New York: McGRAW-HILL.

Efron, B. (1979). Bootstrap Methods: Another look at the Jackknife. *The Annals of Statistics*. 7, 1, 1-26.

Efron, B. and Tibshirani, B. (1993). An Introduction to the Bootstrap. Chapman and Hall. New York.

- Etkin DS (2000). Worldwide analysis of oil spill cleanup cost factors. Proceedings of the 23rd Arctic and Marine Oil spill Program (AMOP) Technical Seminar; Environment Canada; Ottawa, Ontario, Canada. 161-174.
- Faber, M. H. (2002). Risk-Based Inspection: An Introduction. Structural Engineering International. 12, 186-195.
- Great Britain. Health and Safety Executive. (2002). Guidelines for use of statistics for analysis of sample inspection of corrosion. Sudbury: HSE Books.
- Gross, S. (1980). Median estimation in sample surveys. Proceedings of the Section of Survey Research Methods. American Statistical Association. 181-184.
- Hobbs, D. and Ku, A. (2002). Statistical consideration for determining extend of piping inspections for RBI or API-570 driven inspections. ASME Pressure Vessels and Piping Conference. 167-172. Vancouver, British Columbia, Canada.
- Hobbs, D. and Ku, A. (2002). Statistical consideration for determining extend of piping inspections for RBI or API-570 driven inspections. ASME Pressure Vessels and Piping Conference. 167-172. Vancouver, British Columbia, Canada.
- Jarrah, A., Bigerelle, M., Guillemot, G., Najjar, D., Iost, A. and Nianga, G.M. (2011). A generic statistical methodology to predict the maximum pit depth of a localized corrosion process, Corrosion Science. 53, 8, 2453e2467.

Joseph, L. and Bélisle, P. (1997). Bayesian sample size determination for normal means and differences between normal means. *The Statistician*. 46, 2, 209-226.

Kallen, M.J. (2002). Risk-based inspection in the process and refining industry. Master thesis, Faculty of Information technology and Science, technical University of Delft, delft, The Netherlands.

Kallen, M.J. and Noortwijk, J.M. (2004). Optimal inspection and replacement decisions for multiple failure modes. *Probabilistic Safety Assessment and Management (PSAM7 ESREL'04): Proceedings of the 7th International Conference on Probabilistic Safety Assessment and Management*, Berlin, Germany.

Khalifa, M., Khan, F. and Haddara, M. (2009). Optimal selection of non-destructive inspection technique for welded components. *The British institute of non-destructive testing. Insight*. 51, 4, 192-200.

Khalifa, M., Khan, F. and Haddara, M. (2012a). A Methodology For Calculating Sample Size To Assess Localized Corrosion of Process Components. *Journal of Loss Prevention in the Process Industries*. 25, 70-80.

Khalifa, M., Khan, F. and Haddara, M. (2012b). Bayesian sample size determination for inspection of general corrosion of process components. Journal of Loss Prevention in the Process Industries, 25, 218-223.

Khan, F., Haddara, M. and Khalifa, M. (2012). Thermal power plant performance, Chapter 10: Risk-based inspection and maintenance (RBIM) of power plants. DOI: 10.1007/978-1-4471-2309-5-10. In press.

Khan, F. and Howard, R. (2007). Statistical approach to inspection planning and integrity assessment. Journal of Non-destructive Testing and Condition Monitoring. 49, 1, 26-36.

Khan, F. and Howard, R. (2007). Statistical approach to inspection planning and integrity assessment. Non-destructive testing and condition monitoring. 49, 26-36.

Khan, F.I., Haddara, M.M., and Bhattacharya, S.K. (2006). Risk-Based Integrity and Inspection Modeling (RBIIM) of Process Components/System. Risk Analysis. 26, 203-221.

Khan, F. and Howard, R. (2007). Statistical approach to inspection planning and integrity assessment. Insight - Non-Destructive Testing and Condition

Monitoring Insight - Non-Destructive Testing and Condition Monitoring. 49, 1, 26-36.

Khan, F.I. and Abbasi, S.A. (2000). Analytical simulation and PROFAT II: A new methodology and a computer automated tool for fault tree analysis in chemical process industries, Journal of Hazardous Materials. 75, 1-27.

Khan, F.I. and Haddara, M. (2003). Risk-based maintenance (RBM): a quantitative approach for maintenance/ inspection scheduling and planning. Journal of Loss Prevention in the Process Industries. 16, 561-573.

Khan, F.I., Haddara, M. (2004). Risk-based maintenance (RBM): a new approach for process plant inspection and maintenance. Process Safety Progress. 23, 4, 252-265.

Kowaka, M., Tsuge, H., Akashi, M., Katsumi, M. and Ishimoto, H. (1984). Introduction to life prediction of industrial plant materials: Application of extreme value statistical method for corrosion analysis. The Japan society of corrosion engineers.

Krishnasamy, L., Khan, F., Haddara, M. (2005). Development of a risk-based maintenance (RBM) strategy for a power-generating plant. Journal of Loss Prevention in the Process Industries. 18, 2, 69-81.

- Laycock, P.J. (1990). Extrapolation of extreme pit depths in space and time. Journal of the Electrochemical Society. 137, 1, 64-69.
- Lees, F.P. (1996). Loss Prevention in the Process Industries, London: Butterworths.
- Li, H. (2007). Hierarchical Risk Assessment of Water Supply Systems. Submitted for the Degree of Doctor of Philosophy, Loughborough University, UK.
- Misewicz, D., Smith, A.C., Nessim, M. and Playdon, D. (2002). Risk based integrity project ranking. Proceedings of IPC'02, IPC2002-27214.
- Nessim, M. A., Stephens, M. J., Zimmerman, T. J. E. (1995). Risk based maintenance planning for offshore pipelines. Proceedings of the Annual Offshore Technology Conference. 2, 791-800.
- Paris, P.C. and Erdogan, F., (1963). Critical Analysis of Crack Propagation Laws. Basic Eng. 85, 528-534.
- Pezeshk, H. (2003). Bayesian techniques for sample size determination in clinical trials: A short review. Stat Methods Med Res Statistical Methods in Medical Research. 12, 6, 489-504.

Pressure Systems Safety Regulations, PSSR (2000). Safety of pressure systems. Approved Code of Practice (ACoP). SI-2000-128. The Health and Safety Executive (HSE).

RAC (2002). Non-electric components reliability data, Center for Reliability Assessment, New York.

Ragab, Abel-Rahman and Bayoumi, Salah Eldin. (1999) Engineering Solid Mechanics Fundamentals and Applications Book. Boca Raton, Fl.: CRC Press, ISBN 0849316073.

Sadiq, R, Saint-Martin, E. and Kleiner, Y. (2008). Predicting risk of water quality failures in distribution networks under uncertainties using fault-tree analysis. *Urban Water Journal*. 5, 4, 287-304.

Sahu, S.K., and Smith, T.M. (2006). A bayesian method of sample size determination with practical applications. *Journal of the Royal Statistical Society: Series A (Statistics in Society)*. 169, 2, 235-253.

Santosh, T.V., Vinod, G., Shrivastava, O.P., Saraf, R.K., Ghosh, A.K., & Kushwaha, H.S. (2006). Reliability analysis of pipelines carrying H<sup>2</sup>S for risk based inspection of heavy water plants. *Reliability Engineering and System Safety*. 91, 163-170.

Schneider, C.R.A., Muhammed, A. and Sanderson, R.M. (2001). Predicting the remaining lifetime of in-service pipelines based on sample inspection data. *Insight: Non-destructive testing and corrosion monitoring*. 43, 2, 102-104.

Shibata, T. (1991). Evaluation of corrosion failure by extreme value statistics. *ISIJ International*. 31, 2, 115-121.

Stamey, J. D., Young, D.M., and Bratcher, T.L. (2006). Bayesian sample-size determination for one and two poisson rate parameters with applications to quality control. *Journal of Applied Statistics*. 33, 6, 583-594.

The Health and Safety Executive, HSE (2002). Guidelines for the use of statistics analysis of sample inspection of corrosion. Research Report 016. Cambridge, U.K.: TWI.

Thodi, P., Khan, F. and Haddara, M. (2009). The selection of corrosion prior distributions for risk based integrity modeling. *Stochastic Environmental Research and Risk Assessment*. 23, 6, 793-809.

Vaurio, J.K. (1995). Optimization of test and maintenance intervals based on risk and cost. *Reliability Engineering and System Safety*.

Vesely, W.E., Goldberg, F. F., Roberts, N.H. and Haasl, D.F. (1981). Fault tree handbook. U.S. Nuclear Regulatory Commission, NUREG-0492, Washington, DC.

Wang, W.D. (2006). Extreme value analysis of heat exchanger tube inspection data. Proceedings of PVP2006-ICPVT-11 ASME Pressure Vessels and Piping Division Conference. Vancouver, BC, Canada.

Wilcox, C.R. and Ayyub, M.B. (2003). Uncertainty Modeling of Data and Uncertainty Propagation for Risk Studies. IEEE Proceedings on Uncertainty Modeling and Analysis. 184-191.

Wintle, J.B., Kenzie, B.W., Amphlett, G.J. and Great Britain. (2001). Best practice for risk based inspection as a part of plant integrity management. Great Britain, Health and Safety Executive.

Yee, R.D., (1997). Ship Structure Committee. Coast Guard, Fleet Technology Limited., & MSEI (Firm). United States. Guide to damage tolerance analysis of marine structures. [Washington, D.C.]; Springfield, VA: Ship Structure Committee, SSC-402.

Zhao, J.P. (2009). Risk-Based Inspection Analysis for High-Pressure Hydrogenation Cracking Unit. *Journal of Pressure Vessel Technology*. 131, p24503.

Zhou, T. and Chan, Tommy H.T. (2007). Hot spot stress analysis of fatigue for Tsing Ma Bridge critical members under traffic using finite element method. *Key Engineering Materials*. 353, 925-928.

